Nanoliter Droplet Microarrays Combined with Impedance Spectroscopy and Sandwiching Method for Advancements in Miniaturized Cell Culture and Screening

Zur Erlangung des akademischen Grades eines
DOKTORS DER NATURWISSENSCHAFTEN
(Dr. rer. nat.)

von der KIT-Fakultät für Chemie und Biowissenschaften
des Karlsruher Instituts für Technologie (KIT)

genehmigte

DISSERTATION

von

M. Sc (Eng). Meijun Zhou

Referent. Prof. Dr. Pavel A. Levkin

Korreferent. Prof. Dr. Lennart Hilbert

Tag der mündlichen Prüfung. 15.07.2024

Eidesstattliche Erklärung

Hiermit versichere ich, dass ich die vorliegende Arbeit selbständig verfasst und keine anderen als die angegebenen Quellen und Hilfsmittel verwendet, sowie Literaturzitate kenntlich gemacht habe. Die Satzung des Karlsruher Instituts für Technologie (KIT) zur Sicherung guter wissenschaftlicher Praxis wurde beachtet. Die elecktroische Version der Arbeit stimmt mit der schriftlichen überein und die Abgabe und Archivierung der Primärdaten gemäßAbs. A (6) der Regeln zur Sicherung guter wissenschaftlicher Praxis der KIT beim Institut ist gesichert.

Ort und Datum Unterschrift

Abstract

This dissertation presents two novel methods for cellular analysis and cultivation on nanoliter droplet microarrays. First, using impedance spectroscopy for drug response analysis in nanoliter droplets; and second, using sandwiching method for controlled manipulation of nanoliter droplet and long-term cell culture on nanoliter droplet arrays.

The first part of the research introduces an innovative technique that combines Droplet Microarray (DMA), a platform based on hydrophilic spots surrounded by super-hydrophobic borders, in which nanoliter droplets can be precisely formed on hydrophilic spots, with impedance spectroscopy to provide a novel method for label-free and real-time analyzing cellular responses to drug treatments. This method determines cell behavior by measuring the impedance produced when cells attach on the surface of electrodes. This method is the first successful attempt to miniaturize cell bioelectrical signaling to nanoliter volumes, providing a method that captures small changes in cellular behavior and viability and measurement of drug toxicity at the cellular level.

The second part of the study focuses on using innovative sandwiching method to achieve controlled and parallel manipulation of nanoliter droplets containing cells. Using sandwiching method, I address common challenges in culturing cells at nanoscale volumes, such as nutrient supply, waste removal, and long-term maintenance of cell viability, and I can easily culture adherent and suspension cells up to 7 days in nanoscale volumes. Additionally, I have successfully performed 2D-3D cell co-cultures on the same DMA by transferring spheroids between droplets in parallel within seconds without causing cell damage. Furthermore, I demonstrate sandwiching method can perform sampling

extract from DMA without any damage of cells by using lactate dehydrogenase (LDH) to detect extracellular toxicity. This technique enhances the functionality of DMA, enabling long-term cell culture and high-throughput manipulation and sampling for screening purposes within nanoliter droplets.

In summary, this work is focused on developing novel methods for cell-based screening applications on DMA chips. First, I have developed a novel method - electrode Droplet Microarray (eDMA), which combines nanoliter droplet microarrays and impedance spectroscopy for dynamic cell analysis. This study presents the first demonstration of continuous impedance monitoring within nanoliter droplets. It can detect subtle changes in cellular behavior and viability, and measure drug toxicity at the cellular level. Second, I established and validated a sandwiching method, which is used to manipulate nanoliter droplets in high throughput and parallel manner. It improves the usability of DMA, allowing label-free replacement of cell culture media for long-term culture, high-throughput and non-invasive sampling from the droplets and transfer of spheroids. The established in my work methodologies pave the way to novel applications of the DMA platform, which is by itself enabling technology for highly miniaturized cell-based screenings, unique for screening of cells of limited availability.

Zusammenfassung

Diese Dissertation stellt zwei neue Methoden zur Zellanalyse und -kultivierung auf Nanolitertröpfchen-Mikroarrays vor. Erstens die Verwendung von Impedanzspektroskopie zur Analyse der Arzneimittelreaktion in Nanolitertröpfchen; und zweitens die Verwendung der Sandwich-Methode zur kontrollierten Manipulation von Nanolitertröpfchen und zur langfristigen Zellkultivierung auf Nanolitertröpfchen-Arrays.

Der erste Teil der Forschung stellt eine innovative Technik vor, die Droplet Microarray (DMA) – eine Plattform auf Basis von hydrophilen Punkten, die von superhydrophoben Rändern umgeben sind, und bei der Nanolitertröpfchen präzise auf hydrophilen Punkten gebildet werden können – mit Impedanzspektroskopie kombiniert, um eine neuartige Methode zur markierungsfreien und Echtzeitanalyse zellulärer Reaktionen auf Arzneimittelbehandlungen bereitzustellen. Diese Methode bestimmt das Zellverhalten durch Messen der Impedanz, die erzeugt wird, wenn Zellen an der Oberfläche von Elektroden haften. Diese Methode ist der erste erfolgreiche Versuch, die bioelektrische Signalgebung von Zellen auf Nanolitervolumina zu miniaturisieren und bietet eine Methode, die kleine Änderungen im zellulären Verhalten und der Lebensfähigkeit erfasst und die Arzneimitteltoxizität auf zellulärer Ebene misst.

Der zweite Teil der Studie konzentriert sich auf die Verwendung einer innovativen Sandwich-Methode zur kontrollierten und parallelen Manipulation von Nanolitertröpfchen, die Zellen enthalten. Mit der Sandwich-Methode bewältige ich gängige Herausforderungen bei der Kultivierung von Zellen in Nanovolumina, wie Nährstoffversorgung, Abfallbeseitigung und langfristige Aufrechterhaltung der

Zelllebensfähigkeit, und ich kann anhaftende und suspendierte Zellen problemlos bis zu 7 Tage in Nanovolumina kultivieren. Darüber hinaus habe ich erfolgreich 2D-3D-Zell-Kokulturen auf derselben DMA durchgeführt, indem ich Sphäroide innerhalb von Sekunden parallel zwischen Tröpfchen transferierte, ohne Zellschäden zu verursachen. Darüber hinaus zeige ich, dass die Sandwich-Methode Probenextrakte aus DMA entnehmen kann, ohne Zellen zu schädigen, indem sie Lactatdehydrogenase (LDH) verwendet, um extrazelluläre Toxizität zu erkennen. Diese Technik verbessert die Funktionalität von DMA und ermöglicht eine langfristige Zellkultur und eine Manipulation und Probenentnahme mit hohem Durchsatz für Screeningzwecke innerhalb von Nanolitertröpfchen.

Zusammenfassend konzentriert sich diese Arbeit auf die Entwicklung neuartiger Methoden für zellbasierte Screening-Anwendungen auf DMA-Chips. Zunächst habe ich eine neuartige Methode entwickelt – das Elektroden-Droplet-Microarray (eDMA), das Nanoliter-Droplet-Microarrays und Impedanzspektroskopie für die dynamische Zellanalyse kombiniert. Diese Studie präsentiert die erste Demonstration einer kontinuierlichen Impedanzüberwachung innerhalb von Nanoliter-Tröpfchen. Sie kann subtile Veränderungen im zellulären Verhalten und der Lebensfähigkeit erkennen und die Arzneimitteltoxizität auf zellulärer Ebene messen. Zweitens habe ich eine Sandwich-Methode entwickelt und validiert, mit der Nanoliter-Tröpfchen mit hohem Durchsatz und parallel manipuliert werden können. Sie verbessert die Benutzerfreundlichkeit von DMA und ermöglicht den markierungsfreien Austausch von Zellkulturmedien für die Langzeitkultur, die durchsatzstarke und nichtinvasive Probenentnahme aus den Tröpfchen und die Übertragung von Sphäroiden. Die in meiner Arbeit entwickelten Methoden ebnen den

Weg für neuartige Anwendungen der DMA-Plattform, die selbst eine Technologie für hochminiaturisierte zellbasierte Screenings ermöglicht, die einzigartig für das Screening von Zellen mit begrenzter Verfügbarkeit ist.

Acknowledgments

I have many people to thank during my years of working and living in Germany. The past few years in Germany have been the most special experiences for me in my life of more than 20 years. This experience made me stay away from my motherland, hometown, and relatives for the first time, and came to Germany to study and work alone. In the city of Karlsruhe, Germany, I experienced the cultural differences and enthusiasm of different countries, and I also met many people who deserve my gratitude.

Firstly, I would like to express my deepest gratitude to my two supervisors. Prof. Dr. Pavel Levkin and Dr. Anna Popova. Thanks to Pavel for giving me the opportunity to work at KIT. Pavel being a remarkably diligent and aspirational professor, made me realize the value of hard work and progress through his expectations. Anna is a kind and patient person, always ready to assist even during her holidays, she is an ideal supervisor and friend. Their guidance, support, and expertise provided invaluable assistance throughout my research process. Their constant encouragement was crucial in overcoming the challenges I faced during my PhD career.

Next, I would like to extend my profound gratitude to Dr. Heinz-Georg Jahnke from the Centre for Biotechnology and Biomedicine (BBZ), University of Leipzig. His collaborative efforts, invaluable support, insightful suggestions, and profound expertise have been instrumental in advancing my work.

Then, I would like to gratitude to my friends and colleagues. Thanks to Dr. Mandsberg Nikolaj and Joaquin E. Urrutia Gomez for their warm assistance and encouragement throughout my works and life. I am very thankful to Sida Liu, Yuliang Shao, Zhenwu Wang, Lutong Lu, Razan El

Khaled El Faraj, Vania Tanda Widyaya, Julián Serna, Julius von Padberg, Maryam Salarian and Charlotte Luchena for creating a pleasant and supportive work environment. During all of the time in this group was both enjoyable and inspiring. To all my friends and colleagues, mere words fall short of expressing my gratitude. Your collective support and friendship have been vital to my life, and I am forever grateful for your presence and influence. Thank you for everything.

I would like to extend my special thanks to my parents, for their love, sacrifice, and endless support that have made me who I am today. Although they cannot give me professional help on my project, they will always be there for me. They are always behind me selflessly support me, encourage me, and believe in me. Their endless patience and understanding are my strong backing, and their trust in my abilities is the source of motivation for me to keep moving forward. Mom and Dad, I love you. To my husband, it was fate that made us meet on the other side of the China in Karlsruhe. It was meeting him that made my life studying abroad more colorful. I thank him for his companionship and care in my life, so that I can focus on my project. His support and encouragement played an important role in my doctoral career.

Lastly, I would like to thank Chinese scholarship count (CSC) for helping me study abroad so that I don’t have to worry about living expenses.

Table of Contents

List of figures

List of tables

List of Abbreviations

DOX	Doxorubicin
eDMA	electrode Droplet Microarray
DMA	Droplet Microarray
EIS	Electrochemical Impedance Spectroscopy
MEA	Microelectrode Array
LDH	Lactate Dehydrogenase
HTS	High-Throughput Screening
HEMA-co-EDMA	Hydroxyethyl Methacrylate-co-Ethylene Dimethacrylate
DMEM	Dulbecco's Modified Eagle Medium
FBS	Fetal Bovine Serum
P/S	Penicillin/Streptomycin
RPMI	Roswell Park Memorial Institute (medium)
ETO	Etoposide
HeLa CCL2	Human cervical cancer cell
HEK 293T	Human Embryonic Kidney 293 cells with SV40 T-antigen
SU-DHL4	A cell line derived from human diffuse large B-cell lymphoma
CB	Cell Buffer
SG-Polymer	Specific Gravity Polymer
PEG-Link	Polyethylene Glycol Link
EP tube	Eppendorf Tube

Chapter 1. Introduction

1.1 Cell culture and cell analysis in biomedical research

1.1.1 Concept and development

Cell culture is the process of growing and maintaining cells outside their natural environment, usually in laboratory conditions[1]. This technology involves providing cells with the necessary nutrients, growth factors, and environmental conditions to support their proliferation and survival in vitro[2-4]. Cell culture was developed in the early 20th century with the purpose of providing a controlled environment for studying the behavior of animal cells[5]. The main milestones in cell culture are shown in Figure 1[6]. This technology enables researchers to observe cellular responses and functions without the complex systems effect that occur within an organism[7]. By isolating cells and growing them under laboratory conditions, scientists have gained new insights from cells, which are widely used in cell physiology, metabolism, and pathology. There are several cell sources to extract primary cells using tissues, embryos, eggs and blood (Figure 2)[8]. Cell culture method improves our understanding of fundamental biological processes and paves the way for major discoveries in areas such as pharmacology, toxicology, and regenerative medicine.

Cell analysis is the process of examining and evaluating various characteristics or properties of cells. This can include a wide range of techniques and methods used to study aspects such as cell structure, function, behavior, and interactions with other cells or their environment[8]. Cell analysis is fundamental in many fields of biology, biotechnology, and medicine.

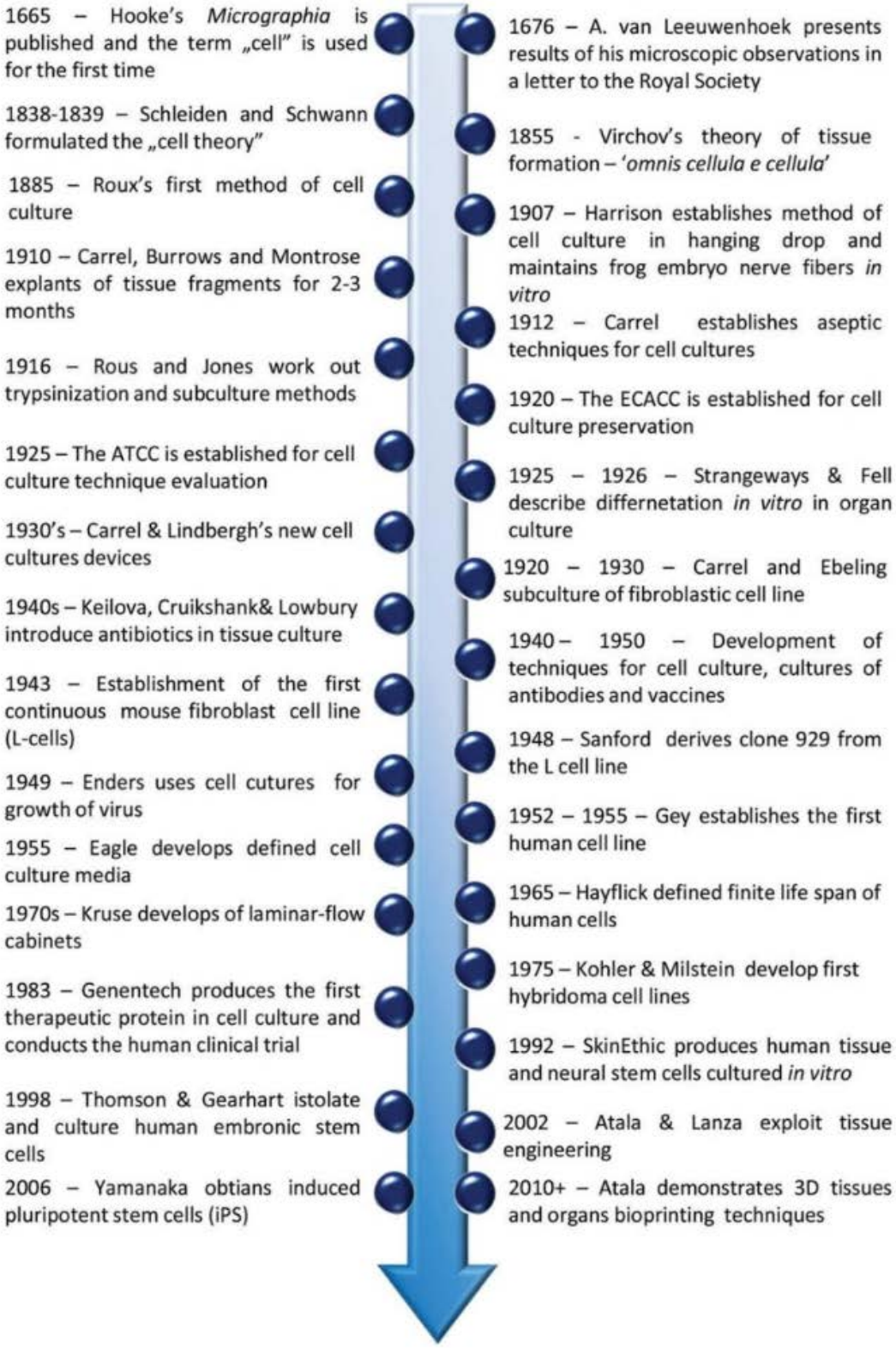

Figure 1. Timeline of cell culture milestones. The figure is reproduced from [6].

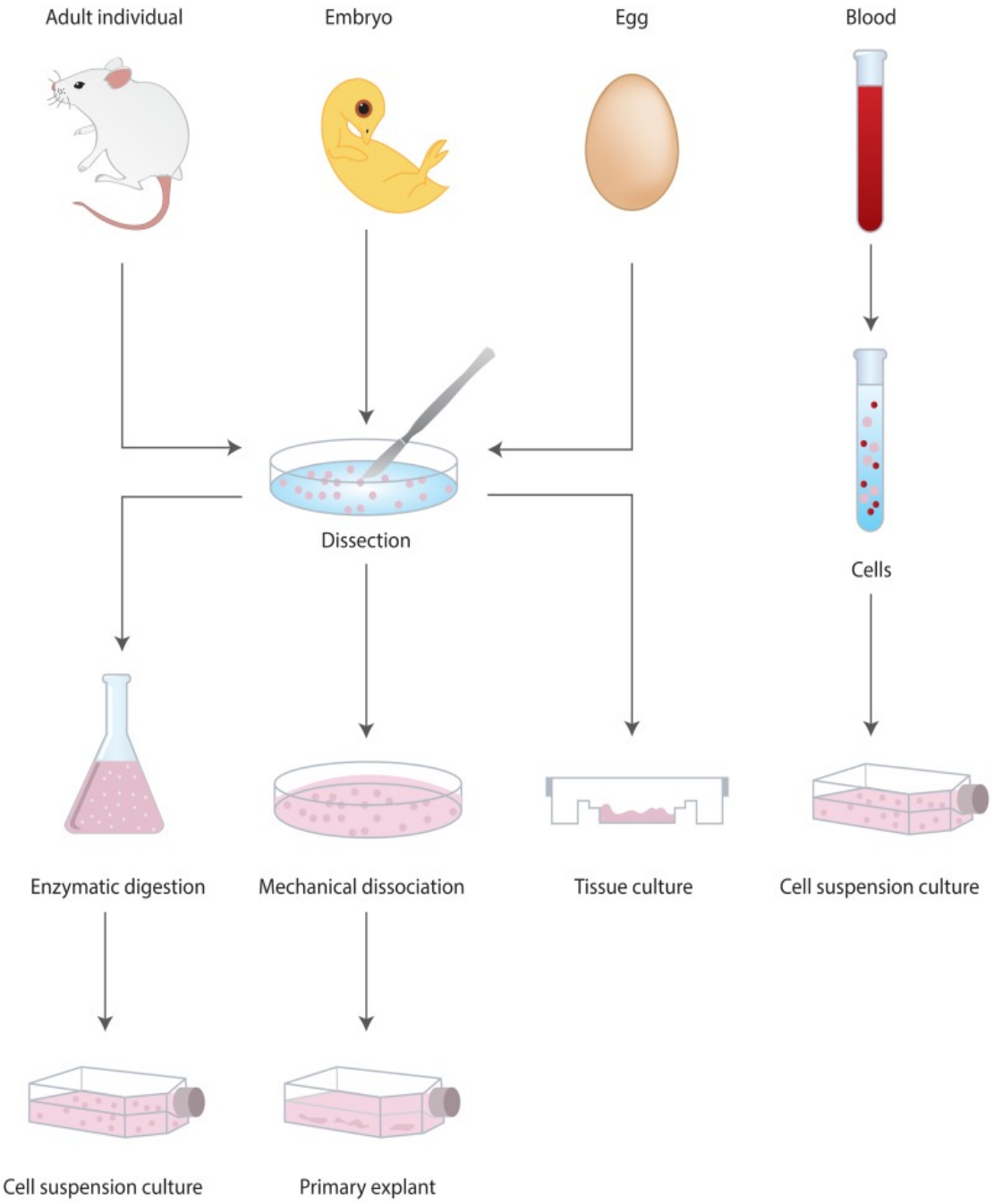

Figure 2. Main sources of cells for in vitro cell cultures. The figure is reproduced from [8].

1.1.2 Technical advantages

Nowadays, in the field of biology, there are many cell analysis techniques that reveal the complex molecular and cellular mechanisms behind various human health conditions. These methods, from flow cytometry[9-11] and microscopy[12-14] to advanced genomic and proteomic technologies[15-17], have become necessary tools in biological research.

For example, flow cytometry allows for rapid quantification and classification of cells based on specific markers by facilitating studies on immune responses[18-20] and cancer cell populations[21-23]. This technique involves passing cells in a fluid stream through a laser beam, where their fluorescence and light scattering properties are analyzed (Figure 3). By detecting fluorescently labeled antibodies or other markers, flow cytometry can identify different cell types and characterize their properties[9,10,24].

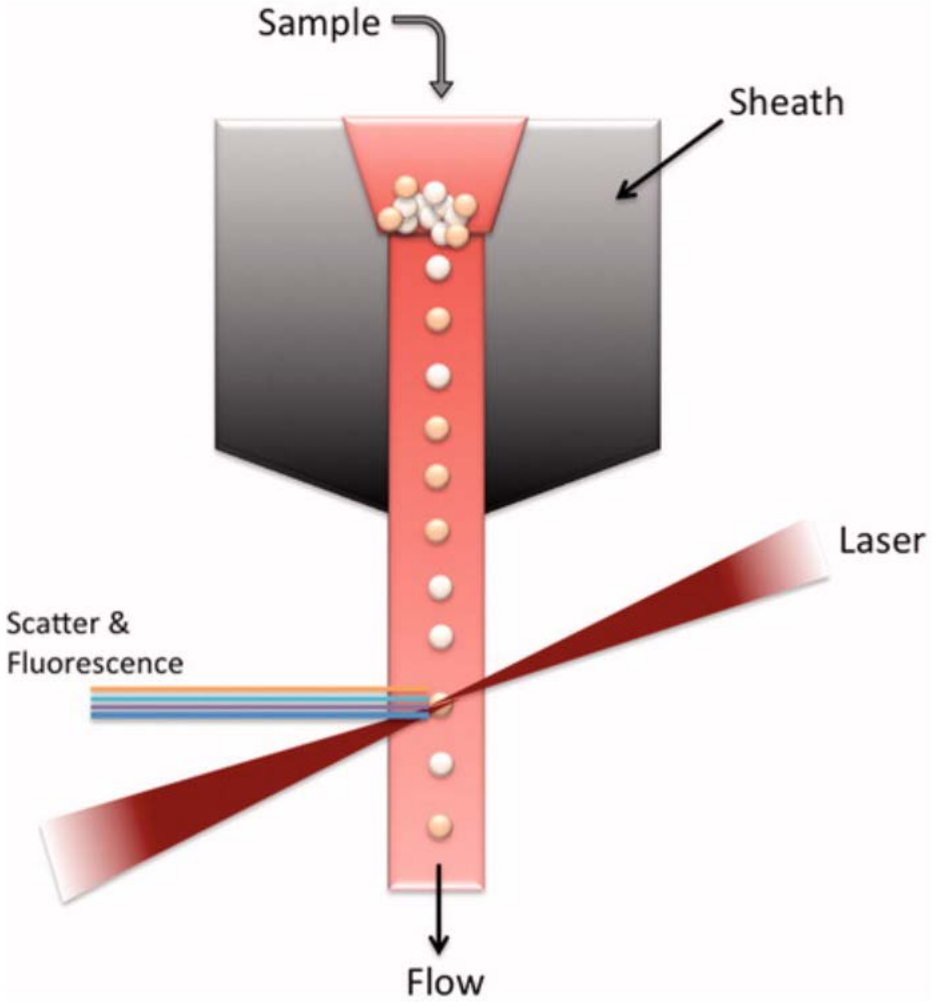

Figure 3.The underlying working principle of a flow cytometer. Flow cytometry works by arranging sample cells into individual streamers that pass sequentially through a laser beam, causing the sample to scatter light and emit fluorescence. A detector captures these light signals and converts them into electronic signals to analyze the size of the cells, their internal structure, and the presence of markers. The figure is reproduced from [10].

Fluorescence microscopy is a powerful imaging technique that can visualize biological structures and processes at the cellular and subcellular levels. It works on the principle of fluorescence, whereby specific molecules called fluorophores emit longer wavelength light after being

excited by a shorter wavelength light source, such as a laser or filtered light[10,24,25]. The emitted fluorescence is then captured and visualized using specialized detectors and imaging systems[24]. It has ability to selectively label and visualize specific molecules or structures in biological samples. By using fluorescent probes, antibodies, or genetically encoded fluorescent proteins, researchers can locate and visualize specific cellular components, such as proteins[26], DNA[27], or organelles[28], with high specificity and sensitivity. This enables detailed studies of cell morphology, dynamics, and interactions in living or fixed samples[29,30].

All in all, the cell analysis techniques involve visual observation using microscopy to measure cellular components or activities, flow cytometry for analyzing cell populations, molecular biology methods to study gene expression or signaling pathways, and various imaging technologies to visualize cellular processes in real-time or at a molecular level[8]. The goal of cell analysis is to gain insights into cellular biology, understand disease mechanisms, develop new therapies, and improve diagnostic methods.

1.1.3 Technical challenges

Although traditional cell culture and analysis methods have made great contributions to biological research, they still have some limitations.

One of the main challenges is that traditional techniques are not sufficient to meet the demands of screening the thousands of available chemical compounds, which limits the number of experiments that can be performed simultaneously. This limitation can significantly slow down the research process, especially in the context of drug screening, where millions of compounds are needed to be evaluated for their therapeutic potential and indicate throughput still can be increased to cover the demand

on screening of all these available chemical compounds.

In addition, traditional cell culture methods often require relatively large quantities of reagents and samples, which increases costs and complicates the handling of precious or rare biological materials[31].

These challenges suggest that the urgent need for a high-throughput research method capable of analyzing cell cultures in smaller volumes in comparison with standard multi-well plates for using less regents, thereby saving costs, while achieving higher throughputs, enhances the efficiency and effectiveness of the experiments. Although traditional plates, such as the 6, 12, 24, 48, 96, 384, and 1536-well plates, offer varying capacities ranging from milliliters to microliters, there is an urgent need for a method that can operate in even smaller volumes (nanoliters) to enhance efficiency and reduce reagent usage.

1.2 High-throughput Screening (HTS)

1.2.1 The concept of HTS

High-throughput screening (HTS) is an important method in current biomedical research, facilitating the rapid evaluation of the biological or biochemical activity of a large number of compounds under standardized conditions. It is a mechanized process that allows researchers to test millions of chemicals, genetic modifications, or pharmacological perturbations in a remarkably short time. By performing these tests in a parallel fashion, HTS dramatically accelerates the pace at which a potential new drug, gene, or protein function can be identified and understood[32-37]. The essence of HTS lies in its ability to provide a comprehensive overview of the interactome of biological targets within the cellular or molecular landscape, offering a panoramic view of potential therapeutic or functional candidates.

1.2.2 Technical Advantages

HTS is a powerful technique widely used in drug discovery and various biological research applications. Here are some of the key advantages of HTS.

High efficiency and speed in evaluating vast arrays of samples. HTS allows for the rapid testing of thousands to millions of compounds in a relatively short period. For instance, a study used HTS to screen of hundreds of thousands of compounds for development of new targeted cancer drugs, which indicated HTS's efficiency in drug discovery processes[38].

Integration with other technologies. HTS can be combined with other technologies, such as fluorescence and artificial intelligence, to enhance data analysis and predict the biological activity of compounds more accurately. For example, the fluorescence-activated droplet sorting (FADS) technique, which combines HTS and fluorescent microfluidic technique. It involves the manipulation and sorting of droplets within a microfluidic device based on their fluorescence signals, which presents a fully automated system for optimizing and monitoring droplet sorting in microfluidic screens, achieving high throughput and minimizing false positives. This technique illustrates HTS flexibility in combination with other technologies [39,40].

Cost-effectiveness. The efficiency and speed of HTS can lead to significant cost savings in the long term by reducing the time and resources needed for drug development.

1.2.3 Technical challenges

Despite its potential, HTS also faces challenges.

Data management and analysis. The volumes of data generated require complex computational tools for analysis, often requiring significant investments in bioinformatics infrastructure and expertise. A study by Rocke et al. delves into experimental design and analysis for HTS biological assays, emphasizing the importance of statistical methods in handling the vast experimental data generated in drug screening [41].

Technical limitations. Certain targets or pathways may be difficult to screen using HTS due to technical limitations, such as the need for specific detection methods or the difficulty in miniaturizing certain assays. Moreover, the miniaturization of assays can sometimes lead to issues with assay sensitivity and specificity, potentially resulting in higher rates of false positives or negatives. The complexity of biological systems also means that hits identified in vitro may not always translate effectively into in vivo models, necessitating further validation and optimization[42].

The droplet microarray (DMA) technology, developed in our research group enables high-throughput culturing and screening of cells in array of nanoliter droplets, which is a powerful platform to address the challenges of miniaturization on HTS.

1.3 Droplet microarray technology (DMA)

1.3.1 Concept and fabrication

DMA is a type of lab-on-chip technology that allows scientists to handle and analyze very small amounts of liquids using a special surface. This surface is designed with patterns that can hold nanoliter droplets in defined areas, facilitating miniaturization down to nanoliter volumes and thereby achieving higher throughput and efficiency. It can be used to investigate how cells respond to drugs or how different chemicals interact with biomolecules[43-45]. It is used in biology and chemistry for precise

experiments with minimal waste, including phenotypic assessment and gene expression analysis[46], high-throughput formation of miniaturized cocultures[47], high-throughput screening for antimicrobial compounds[48] and pluripotency maintenance proteins[49], screening of embryoid body[50] and stem cells[51-53], miniaturized drug sensitivity and resistance test[54-56] and high-throughput drug synthesis and screening[57].

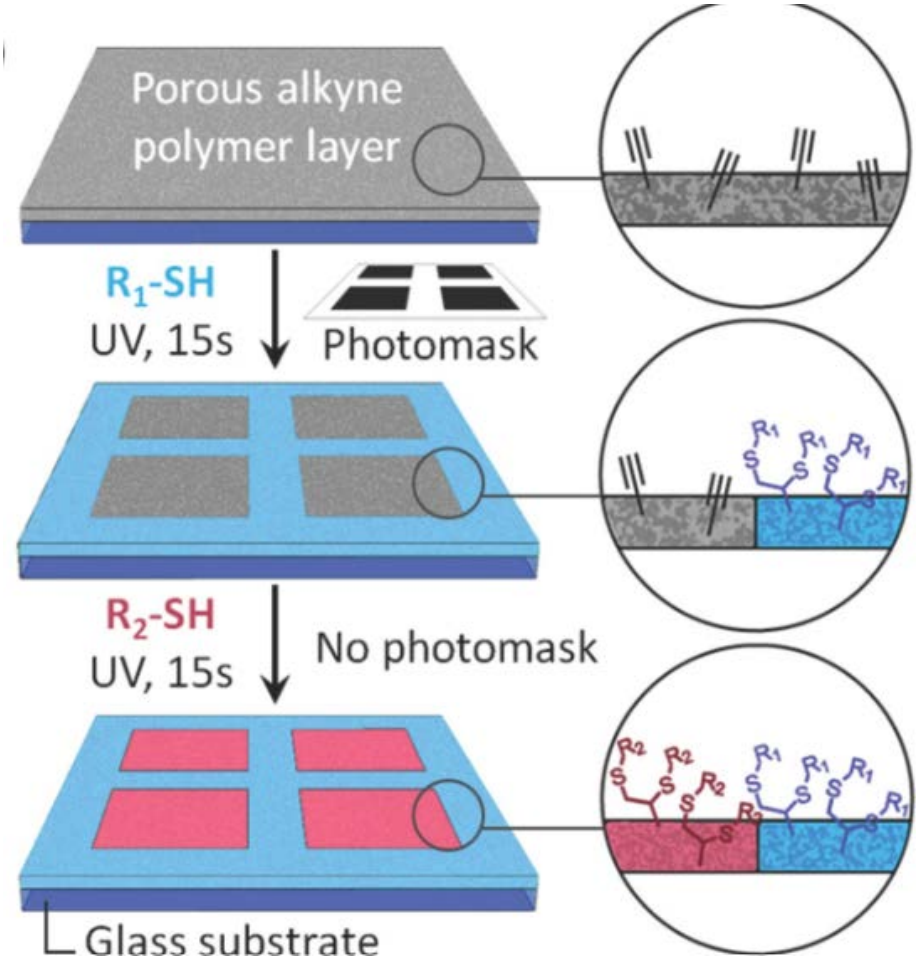

Figure 4. The workflow of superhydrophilic-superhydrophobic micropattern. A photomask and UV light were utilized to introduce superhydrophobic groups into the exposed alkyne regions. Subsequently, the photomask was removed, allowing the remaining alkyne groups to react with a superhydrophilic group. This process resulted in a patterned surface with distinct regions functionalized with superhydrophobic and superhydrophilic groups. The figure is reproduced from [44].

The DMA technology utilizes thiol-yne and thiol-ene click chemistry to engineer surfaces with distinct hydrophilic and superhydrophobic properties. The water contact angle (WCA) measures the angle formed when a water droplet meets a solid surface, indicating the surface's wettability. A superhydrophobic surface has a WCA greater than 150°, signifying a strong repulsion to water[58]. Conversely, a WCA of less than 10° indicates superhydrophilicity, where the water droplet spreads extensively over the surface[59]. Hydrophilic surfaces attract water, while superhydrophobic surfaces repel it, causing water droplets to form with minimal contact area on DMA surface.

In our laboratory, DMA is fabricated to create three types of surfaces. Poly(2-Hydroxyethyl methacrylate-co-ethylene dimethacrylate) (HEMA-EDMA) [60], dendrimer surfaces[61] and nanoparticle surface. For the HEMA-EDMA surface, a porous alkyne polymer layer was generated by modifying glass with HEMA-EDMA. For the nanoparticle surface, the glass surface was silanized with vinyltrimethoxysilane. For the dendrimer surface, glass slides were silanized using triethoxyvinylsilane. The slides are then modified with 1-thioglycerol and subsequently esterified with 4-pentenoic acid, resulting in a dendrimer surface. Finally, the surfaces were modified by photomasking under UV light using *1H,1H,2H,2H*-perfluorodecanethiol (PFDT) and cysteamine hydrochloride, to create superhydrophobic and superhydrophilic surfaces, respectively. The DMA technology was commercialized by Aquarray GmbH since 2018.

The rapid and versatile nature of thiol-yne and thiol-ene reactions allows for precise control of the patterning process, enabling the creation of complex surface designs with tailored wetting behaviors[44]. These surfaces can be used for various liquid types, from organic[62] to aqueous[63], and are applicable for chemistry synthesis and cell-based screenings. The

application of the DMA chips includes drug discovery[36], cellular analysis[64] and chemical synthesis[65], showing its versatility and the critical role it plays in improving our understanding of biological and chemical systems.

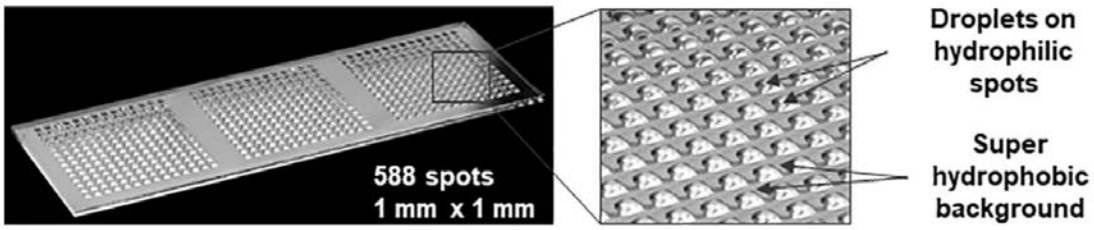

Figure 5. Image of DMA. The figure is reproduced from [36].

1.3.2 Technical advantages

The DMA platform has many advantages compared to traditional multi-well plates, the main advantages include.

Miniaturization. The DMA platform allows to use of nanoscale volume, using less reagents than traditional multi-well plates, saving costs while improving experiment efficiency.

Precise localization. Due to the presence of hydrophilic and hydrophobic regions, droplets are precisely positioned in hydrophilic areas, ensuring accurate localization.

Avoid cross-contamination. The layout of hydrophilic spots separated by superhydrophobic boundaries effectively prevents any crosstalk between adjacent spots on the DMA slide.

Customizable design. Different sized photomasks are used to adjust the dimensions of the DMA platform. This flexibility enables it to meet a variety of experimental requirements and be used in multiple research areas.

High-throughput. DMA platform usually consists of hundreds or

thousands of spots, so it is a high-throughput screening platform.

Cost-effectiveness. The cells, reagents and other experimental materials can be used by nanoscale on DMA, which reduces the cost of materials for experiment.

Broad compatibility. The DMA platform is compatible with a wide array of samples, from biological samples to chemical and material samples.

In conclusion, the innovative design and operational flexibility of the DMA platform makes it a powerful tool in the field of miniaturized and high-throughput analysis, with the potential to accelerate progress in various fields.

1.3.3 Technical challenges

Despite the considerable advantages offered by droplet microarray technology, there remains a significant opportunity for improvement, particularly in the field of real-time cellular monitoring, small droplet evaporation and the manipulation of nanoliter droplets.

The challenge of real-time cellular monitoring. Due to the nanoscale volume of droplets on the DMA, the liquid must be always maintained in a stable humidity chamber, which makes it challenging to achieve real-time monitoring. The integration of impedance spectroscopy with droplet microarray technology represents a promising method for real-time monitoring. Impedance spectroscopy, a technique that measures the electrical properties of cells, can provide non-invasive, real-time insights into cell viability, growth, and differentiation. When combined with the high-throughput and miniaturization capabilities of droplet microarrays. This integration promises to transform cell analysis through dynamic observation.

The challenge of small droplet evaporation. Maintaining long-term experiment in droplets is critical to understanding the long-term effects of drugs and disease progression over time. Traditional cell culture methods can be used for long-term cell experiment due to larger volumes and possibility of automated medium exchange. However, due to the nanoliter volume of DMA, the fast evaporation rate, and the difficulty of observing change of long-term experiment. This limits the applicability of the DMA platform for long-term cell experiment. To extend the application spectrum of DMA, there is an urgent need for a novel method to manipulate liquid on DMA, this method has potentially transformed our traditional approach to long-term cell studies.

The challenge of manipulation of nanoliter droplets. Compared with other culture platforms such as microplates, DMA has clear advantages in scalability and single droplet operation. However, the nanoliter-sized droplets and hundreds and thousands of spots are highly prone to evaporation, posing challenges for manipulating cell cultures and achieving label-free sampling on DMAs are difficult. Furthermore, standard measuring equipment, such as plate readers, is incompatible with DMAs. To broaden the application scope of DMAs, there is an urgent need to develop new methods for effective droplet manipulation on this platform.

1.4 Electrochemical Impedance Spectroscopy (EIS)

1.4.1 The concept of EIS

Electrical impedance spectroscopy (EIS) technology is a powerful analytical technique that is used for real-time monitoring of cell behavior[66], which utilizes a low-frequency alternating current applied across a surface containing cells to monitor changes in voltage drop[67 68]. It involves applying a small amplitude alternating current (AC) to an electrode pair in

solution and measuring the resulting voltage response. The calculated impedance as a function of AC frequency provides detailed information about various processes occurring near the electrode´s surface. As cells attach and spread on the electrodes, the impedance changes[69]. This technique relies on the principle that cells exhibit unique impedance distributions due to their size, shape, membrane properties and intracellular content[70]. EIS is a label-free and non-invasive method that enables monitoring the impedance over time giving real-time insight into cell attachment kinetics and behavior[71].

The integration of EIS with cell studies has opened new pathway in biomedical research, particularly in areas like cytotoxicity assays[72,73], cancer research[74], and tissue engineering[75]. By applying an AC voltage and measuring the resulting impedance, researchers can infer various cellular properties without the need for labeling or invasive procedures, preserving the natural state of the cells[76].

By simulating circuits, I can break down complex electrochemical behaviors into simpler, more understandable components. In bio-impedance analysis, EIS is used to study the electrical properties of biological tissues. Equivalent circuit models can simulate the electrical behavior of cells or tissues, such as the capacitive behavior of cell membranes and the resistance to ion migration inside and outside the cell. This helps in studying changes in cell physiological states and tissue structures. In the EIS equivalent circuits for cells, the following components are commonly included[77,78].

- Resistors, which represent the resistance of the media inside and outside the cell.
- Constant phase element (CPE), which represents the non-ideal

capacitive behavior of cell membranes.

- Capacitors, which represent the ideal capacitive behavior of cell membranes.

1.4.2 Technical advantages

EIS is a powerful tool widely utilized across various fields, particularly in cellular studies. Its application in this domain offers several significant advantages.

Non-invasiveness. EIS measures the impedance of cells attached on electrodes without a need for labeling of the cells and application of harmful agents. This measurement is based on the electrical properties of the cell membrane and the surrounding medium, ensuring that the cellular structure and function remain undisturbed during the analysis[79]. The non-invasive nature of EIS allows for the observation of cellular responses in their native state, providing insights into cellular health, viability, and function without influence associated with invasive techniques.

Real-time monitoring. EIS can continuously measure impedance changes over time, reflecting alterations in cell morphology, adhesion, or layer integrity in response to external stimuli. This continuous data is obtained without disturbing the cells, allowing for the dynamic observation of cellular processes.

Quantitative analysis. The impedance measurements obtained through EIS can be directly correlated with specific cellular properties, such as cell number, size, and membrane integrity. This correlation provides a quantitative description of cellular states and changes, which can be analyzed.

1.4.3 Technical challenges

Although the integration of EIS with cellular studies offers significant advantages, there are significant challenges that need to be addressed.

Complex data interpretation. EIS generates complex data that often require sophisticated models and fitting procedures for accurate interpretation.

Time-consuming measurement. Traditional EIS requires relatively long test times to obtain accurate electrochemical information. In high-throughput screening, this may result in excessively long test cycles, thus limiting its application in large-scale sample studies.

Large volumes of solution. In EIS experiments, it is often necessary to completely immerse the electrode in the solution under test to ensure sufficient electrochemical interaction and accurate measurements. Therefore, a large volume of solution is necessary to ensure complete contact between the electrode and the solution.

In summary, EIS is a technology that combines electrochemical impedance spectroscopy and cell research, allowing us to better understand the complex behavior of cells. This technology has great potential for the future development of all aspects of biomedical research. The development of a miniaturized impedance measurement system is important to address the challenges posed by EIS.

1.5 Microelectrode array (MEA)

1.5.1 The concept of MEA

The concept of a microelectrode array (MEA) revolves around a grid of electrodes printed on a substrate that interfaces with biological cells to

record or stimulate their electrical activity. MEAs are extensively used in cellular electrophysiology to study the electrical behavior of cells, particularly neurons and cardiomyocytes, in a spatially resolved manner[80-82]. This technology facilitates the investigation of electrical signal propagation, network activity, and cellular responses to drugs or environmental changes, making it useful in fields such as neuroscience, cardiology, and drug development[83-85].

EIS is used to measure and record the impedance on MEA. The primary function of EIS is to measure the overall impedance of a sample, reflecting changes in electrochemical properties, rather than detecting electrical signals generated by cells, which can provide insight into cell viability and membrane integrity. MEA directly captures a cell's electrical activity by recording action potentials or other signal transduction at the electrode-cell interface, providing a detailed map of cell electrical activity[86]. Briefly, MEA is a platform that comprises electrodes and utilizes EIS to measure cell signals. EIS is the method employed on the MEA platform to analyze the electrical properties of cells.

Nowadays, MEAs are combined with EIS capabilities to create systems that can simultaneously record action potentials and measure impedance changes, this typical new MEA system consists of dot-like electrodes arranged in two-dimensional grids, which are utilized to detect and record fluctuations in the extracellular field potential (FP) generated by a cell layer adhered to the electrodes[87]. This facilitates a multifaceted approach to studying cellular responses[88], making it valuable in areas like tissue engineering[89,90], drug screening[91-93], and disease modeling [87].

The application of cell studies on MEA, including neuronal network activity, drug screening, toxicology, tissue engineering, disease modeling,

stem cell research.

Neuronal network activity. Understanding the electrical activity and connectivity in neuronal networks is critical for advancing neuroscience research and developing treatments for neurological disorders. For example, MEA technology aids in understanding the cellular basis of physiology in human brain organoids, including the formation, function, and maintenance of networked neuronal circuitry[94].

Drug screening. Assessing the effects of drugs on cell electrical activity. For example, MEAs serve as a robust tool to study disease-specific genotype-phenotype correlations in vitro, especially in hiPSC-derived neurons, facilitating disease phenotyping and drug discovery[95].

Toxicology. Evaluating the toxic effects of substances on cellular electrophysiology. For example, nanomaterial-based MEAs are used for bidirectional brain interfaces in vitro, highlighting their toxicity studies in brain tissues[96].

Tissue engineering. Monitoring the development and integration of engineered tissues. For example, flexible 3-dimensional MEAs are developed for in vitro brain models, enabling the study of brain-like structures and their electrophysiological properties[97].

Disease modeling. Studying disease mechanisms, especially for neurological and cardiac disorders. For example, MEAs are used to record neuronal network activity during short-term microgravity phases, offering insights into the potential impacts of microgravity on neural functions[98].

Stem cell research. Observing differentiation and behavior of stem cells. MEAs are utilized to study the functional development of human pluripotent stem cell (hPSC)-derived and rat neuronal networks, providing

insights into the electrophysiological activity and drug responses of these cells[99].

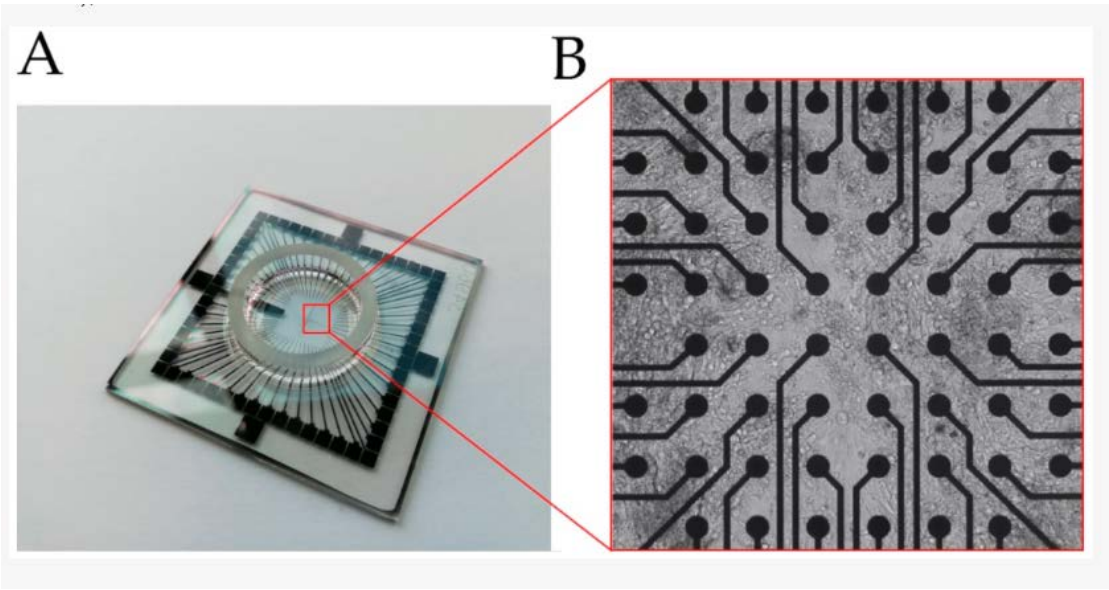

Figure 6. The structure of MEA. (A) Glass multi-/micro-electrode array (MEA) chip used to detect field potential (FP) of cells. (B) Cells seeded on an MEA surface, grown on top of the electrodes (black dots) The figure is reproduced from [87].

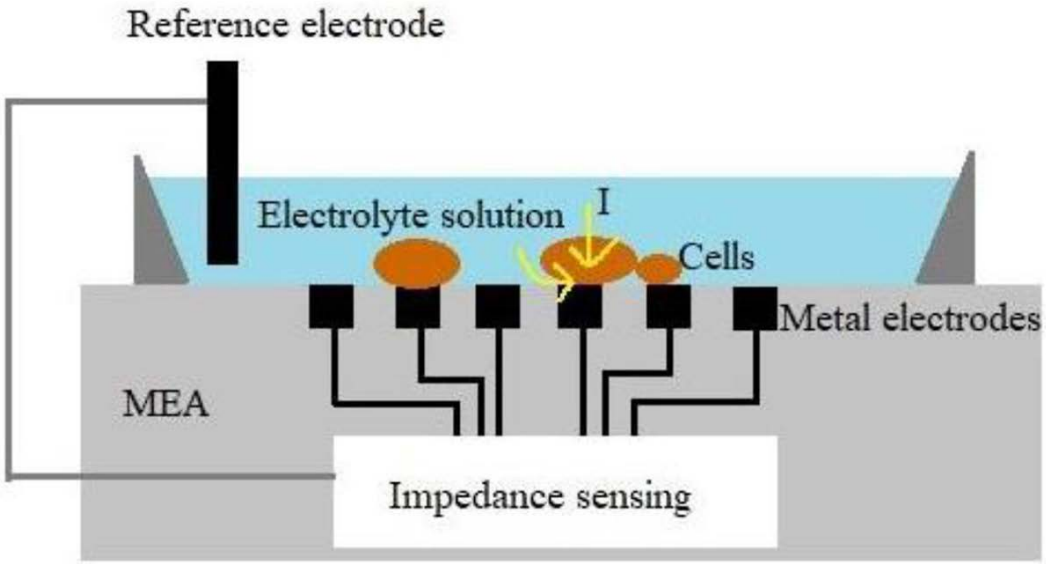

Figure 7. Side view of MEA structure, showing cells attached to microelectrodes. The figure is reproduced from [86].

1.5.2 Technical advantages

MEA platform offers numerous advantages in various scientific and medical research applications, particularly in the study of cell activity.

Non-invasiveness. MEA facilitates non-invasive measurement of extracellular potentials. This minimizes damage to the cells and tissues, preserving their physiological state for accurate and prolonged observation.

Real-time monitoring. MEA enables dynamic, real-time monitoring of electrical activity over extended periods. This is crucial for studying the progression of cellular responses, drug effects, and other time-dependent phenomena.

Long-term viability. MEA platforms often support long-term cell culture and monitoring, allowing researchers to observe chronic effects and long-term changes in cellular activity. This is important for studies on disease progression and long-term drug effects.

1.5.3 Technology challenges

The integration of MEA with cellular systems presents unique challenges but also opens significant opportunities in biological research. Some of the main challenges include ensuring long-term stability and biocompatibility of the MEA when attached to living cells, as well as the complex interpretation of the biological signals obtained.

Future advancements are likely to focus on enhancing the integration of MEA with three-dimensional cell cultures and organoids[100]. This involves improving the resolution and specificity of electrical recordings to capture more detailed and relevant biological information[101]. Additionally, the development of intelligent algorithms for data analysis is crucial for interpreting the complex data sets generated by MEA studies.

The combination of MEA with cellular systems offers a powerful tool for understanding the electrical aspects of cellular function. As this field continues to develop, it is expected to provide new insights into complex biological systems, potentially leading to breakthroughs in therapeutics and diagnostic tools.

Moreover, the integration of droplet microarray technology with EIS and MEA represents a novel approach that combines the strengths of all of platforms. By embedding tinny impedance electrodes within droplet microarray platform, it becomes possible to continuously monitor the electrical properties of cells in individual droplets, enabling real-time tracking of cellular events under various conditions by nanoliter format.

1.6 Drug-dose response in cancer

The exploration of dose-response relationships in cancer drug therapy is very important for oncology research, helping how I understand, develop, and administer anticancer drugs. This critical analysis not only illuminates the drug's therapeutic potential but also highlights the delicate balance between efficacy and toxicity that is crucial in the treatment of cancer.

1.6.1 Concept and development history

The development of the drug-dose response in cancer research can be traced back to Paul Ehrlich's early 20th-century concept of the "magic bullet" [102-104]. This idea has significantly influenced cancer therapy, emphasizing drugs that target cancer cells with minimal damage to healthy tissue. A critical moment was the introduction of methotrexate, a cornerstone of chemotherapy, which demonstrated the importance of dose-response studies in optimizing leukemia[105]. Then, this approach has since been expanded to incorporate personalized medicine and targeted therapies

to address the heterogeneity and adaptability of cancer cells.

Drug potency analysis plays an important role to drug-response study. By studying how different drugs interact with their respective targets at different concentrations, researchers can gain insights into receptor function, signaling pathways, and cellular responses to pharmaceutical intervention. This knowledge facilitates the discovery of new therapeutic targets and the development of drugs with improved potency, selectivity, and safety.

The central to use potency to analysis dose-response is the dose-response curve, usually sigmoidal shaped, indicating the pharmacodynamic relationship between drug concentration and effect[106]. A classic example is the use of doxorubicin, a chemotherapy agent, where low doses may not be sufficient to kill cancer cells, medium doses may be effective in inducing apoptosis, and high doses result in excessive toxicity without increased cancer cell death[107].

Scientists always use the curve's IC50 (the half-maximal inhibitory concentration of drug) to evaluate the dose-response curve of drugs. IC50 indicates the concentration at which a drug inhibits a biological process by 50%. It's crucial in cancer drug-dose response studies as it helps in evaluating the potency of a chemotherapeutic agent against cancer cells. A Lower IC50 value suggests a higher potency, making it a key parameter in drug development and optimization for effective cancer treatment.

1.6.2 Challenges

The study of dose responses to cancer drugs faces many challenges, largely due to the complexity of cancer itself. Tumor heterogeneity between and within individuals makes it difficult to predict how different cancers will respond to the same treatment[108]. Additionally, the dynamic

nature of cancer evolution may lead to drug resistance over time[109]. Except for these factors, it's equally important to minimize harm to healthy cells. This balance is challenging due to the varied response of cancer cells and the risk of adverse effects on normal tissues, making the development of safe and effective treatment protocols complex.

1.6.3 Current detects anticancer drug dose-response methods

The current detects anticancer drug dose-response methods including.

3-(4,5-dimethylthiazol-2-yl)-2,5-diphenyltetrazolium bromide (MTT) assay[110-113]. The MTT assay is simple, cost-effective, and non-radioactive, making it widely used to assess cell proliferation and cytotoxicity. It measures mitochondrial activity as an indicator of cell viability. However, it has limitations, including the inability to differentiate between types of cell death and the potential interference of certain compounds with MTT reagents. Furthermore, it only provides a snapshot of cell viability at a specific time point and lacks dynamic monitoring capabilities.

Fluorescent viability assays[114-117]. Fluorescent viability assays use fluorescent dyes to assess cell health, viability, and metabolic activity. Advantages include high sensitivity, ability to differentiate between live and dead cells, and suitability for high-throughput screening. However, they may be affected by photobleaching and autofluorescence of cells or media, which may complicate data interpretation. In addition, some dyes may be toxic to cells and affect viability after assay. Fluorometric assays also require specific equipment, such as a fluorescence microscope or microplate reader, which may not be readily available in all laboratories.

Flow cytometry[118-120]. Flow cytometry is a powerful technique used

to analyze the physical and chemical properties of cells or particles in a fluid as they pass through a laser. Advantages include the ability to analyze thousands of particles per second, using fluorescent tags to provide detailed information on cell size, granularity and various cell markers. This makes it extremely valuable for detailed cellular analysis including cell counting, biomarker detection, and cell sorting. However, disadvantages include sample preparation complexity, the need for expensive equipment and data analysis expertise, and potential problems following cell viability analysis.

All of the methods for detecting anticancer drug dose-response which immortalized cell lines are exposed to drugs by evaluating cancer resistance indicators including half inhibitory concentration (IC50), resistance index (RI), cytotoxic drug pump-out rate, cell proliferation index, cell growth curve, and apoptosis index. The detailed exploration of dose-response relationships in cancer drug development is a complex process. Dose-response studies are particularly important for the development and use of anticancer drugs because of the need to understand the minimum effective dose of a drug and its toxicity threshold.

My first project-electrode Droplet Microarray (eDMA) aims to explore the development and application of this integrated platform, and deeply explore the technical challenges, method innovations and potential applications of combining droplet microarrays with impedance spectroscopy for cell analysis. The goal is to create a versatile system capable of real-time monitoring and label-free to observe cell dynamics by nanoscale volume, with broad implications for future scientific research and clinical applications.

In summary, the combination of droplet microarray technology and electrochemical impedance spectroscopy offers the birth of a new cell

analysis method, providing a powerful tool for label-free observing changes in cell behavior in real-time.

1.7 Long-term cell culture experiment

Long-term cell culture experiment is an important technique that enables researchers to delve into the extended behaviors, reactions, and differentiation processes of cells in vitro. This approach involves the sustained maintenance and nurturing of cell populations over considerable duration of time, typically lasting Weeks to months, to observe the dynamic cellular processes, genetic expressions, and physiological changes that occur over time[121-125]. It is a method that ensures cells remain viable and functional in vitro for extended periods of time.

1.7.1 The development of long-term culture experiment

The characteristics of long-term culture are continued growth and maintenance of cells over an extended period of time, allowing observation of cell behavior, differentiation pathways, and responses to stimuli that are not possible in short-term cell culture[126-128]. In cell differentiation, maturation of specialized cell types, and the development of complex cellular models such as spheroids, it supports cell viability and function over time without compromising the integrity of the cell structure[129].

The importance of long-term cell culture in revealing the complexities of cellular life is profound, especially in its capacity to mimic the complex of in vivo environments and biological timelines[130]. The extended observation it provides is crucial for studying phenomena such as stem cell differentiation, tissue maturation, and the long-term impacts of drugs or toxins on cellular health[131-134]. By offering a stable platform for cells to grow, divide, and interact, long-term culture facilitates the formation of more physiologically relevant models, including multicellular

spheroids and organoids[135-137]. These models better replicate the structural and functional complexities of tissues and organs within the body, providing invaluable insights into developmental biology, regenerative medicine, and pharmacological testing.

In developmental biology, long-term cell culture allows for the observation of the gradual process of stem cells differentiating into specific cell lineages, revealing the complex signals and mechanisms that guide cell fate decisions. For example, a study by Kleine-Brüggeney et al. demonstrates the use of a 3D hydrogel bead platform for long-term perfusion culture of monoclonal embryonic stem cells, enabling continuous optical analysis of differentiation over extended periods. This method allows for the monitoring of the exit from pluripotency in stem cells, providing valuable insights into the complex signals guiding cell fate decisions[138]. In the field of regenerative medicine, culturing cells over extended periods is essential for growing tissue constructs and organoids that mimic the architecture and functionality of native tissues, offering promising methods for tissue engineering and transplantation. For instance, research has shown that organoids, derived from stem cells, can effectively mimic the complex structure and function of corresponding tissues, offering a new model for improving regenerative medicine outcomes. They use choanocyte organoids for biliary injury, demonstrating the potential of organoids in repairing bile ducts and advancing liver regeneration [139]. Additionally, another study explores the challenges of kidney organoid development for regenerative medicine. The authors note that although significant progress has been made in directing the differentiation of human pluripotent stem cells (hPSCs) toward kidney endpoints, there are still hurdles to overcome before these organoids can be effectively used as replacement therapy. The study emphasizes the need for improved

maturation, vascularization, and reduction of off-target cell populations to enhance the utility of kidney organoids in regenerative medicine applications [140]. Moreover, in pharmacological studies, long-term cell culture plays an important role in assessing the efficacy and toxicity of drug candidates, closely mirroring chronic exposure scenarios common in clinical settings. A recently published study examines the potential of a microfluidic kidney chip for efficient drug screening and nephrotoxicity assessment. This study utilized a co-culture microfluidic model to test drug-induced nephrotoxicity, comparing the viability of renal proximal tubular epithelial cells (RPTECs) on microfluidic chips versus traditional Petri dishes. The results indicated a higher cell viability in the fluidic environment of the microfluidic chip, suggesting its suitability for long-term cell culture and drug function testing, thereby offering a promising platform for pharmacological screenings[141]. Furthermore, another article investigated toxicology's evolving role within the pharmaceutical industry, underscoring the significance of emerging technologies like organs-on-chips and high-content imaging. These innovations are shaping the future of drug safety testing, with a focus on enhancing predictivity and translational relevance to clinical settings. The article emphasizes the utility of such technologies in investigative toxicology, facilitating a deeper understanding of drug-induced toxicities and their mechanisms, which is paramount for long-term pharmacological studies[142].

In summary, long-term cell culture is a cornerstone in cellular biology, offering a method for prolonged dynamics of cellular life and serving as a foundation for advancing our understanding of complex biological systems and their responses to external stimuli.

1.7.2 Technical advantages

Long-term cell culture has many advantages, which are particularly

valuable for various biology research applications. Some of these advantages include.

Consistent cell supply. Long-term cell cultures provide a steady and consistent supply of cells for experiments, reducing the variability that might come from using cells from different sources or at different times.

Study of cellular processes. They enable researchers to study long-term cellular processes, such as differentiation, aging, and the effects of chronic treatments or environmental exposures over extended periods.

Drug development and testing. They are crucial for drug development and testing, providing a platform to observe the long-term effects of drug candidates on cells, including potential toxicities and therapeutic benefits.

1.7.3 Technical challenges

While long-term cell culture offers numerous opportunities for advancing our understanding of cellular dynamics, it also presents a unique set of challenges, particularly when performed in nanoscale droplets[143]. Although the miniaturization of culture environments is beneficial for high-throughput screening and reduced reagent consumption, it also brings a lot of challenges such as rapid evaporation, nutrient consumption, and waste accumulation. These factors can significantly impact cell viability and the accuracy of experimental results.

Evaporation. In nanoscale droplets of limited volume, the rate of evaporation can be accelerated, resulting in changes in the osmotic pressure and concentration of solutes, which can stress cells and ultimately compromise cell viability.

Nutrition and waste management. The limited volume of

nanodroplets limits the amount of nutrients available to cells and their ability to dilute metabolic waste products. The accumulation of waste products and depletion of essential nutrients can create a toxic environment for cells, leading it difficult to grow and maintain cell cultures under conditions suitable for high-throughput analysis. Long-term cell culture in HTS faces issues such as maintaining cellular viability, phenotype stability, and functionality over extended period of time, which is crucial for the reliability of screening outcomes[144].

Consistency and stability. The miniaturization and automation of cell culture for HTS demand innovative approaches to cell seeding, medium exchange, and environmental control to ensure consistency and reproducibility across thousands of wells or droplets. Evaporation, nutrient depletion, and waste accumulation in small volume cultures further compound these challenges, necessitating novel solutions to sustain viable and physiologically relevant cell models for the duration of screening assays.

Physical and mechanical stress. Cells cultured in nanoscale droplets may also experience increased physical and mechanical stress due to high surface-to-volume ratios and the potential for droplets to move or merge.

Addressing these challenges is critical to successfully implement long-term cell culture in nanoscale environments.

1.8 Objectives of this PhD work

This PhD dissertation is dedicated to advancing the field of cellular analysis and culture through the development and application of two novel methods that exploit the potential of nanoliter droplet microarrays. The main objectives of this research are two parts.

1. A novel platform - electrode droplet microarray (eDMA), which integrates nanoliter droplet microarrays with impedance spectroscopy for drug response analysis, enables real-time monitoring, miniaturization, and label-free studies by using our new platform.

Objective 1.1. To design and fabricate an innovative technique that combines nanoliter droplet microarrays with impedance spectroscopy, providing a powerful platform for the real-time and label-free analysis of cellular responses to drug treatments.

Objective 1.2. To characterize and validate the impedance measurement in nanoliter droplets of electrolyte, ensuring robustness and reproducibility of eDMA platform.

Objective 1.3. To optimize the eDMA platform with cells or label-free real-time monitoring of cellular drug response.

2. An innovative sandwiching method for the controlled and parallel manipulation of nanoliter droplets on DMA, allowing for long-term cell culture, parallel and high-throughput droplet removal, transfer of spheroids, and samplings.

Objective 2.1. To address and overcome the inherent challenges associated with different types of culturing cells in nanoliter volumes, specifically focusing on maintaining adequate nutrient supply, efficient waste removal, and sustained cell viability over extended periods of time.

Objective 2.2. To achieve high-throughput and parallel manipulation of spheroids, leading to 2D-3D co-culture on the same DMA.

Objective 2.3. To demonstrate high-throughput and parallel sampling from nanoliter droplets.

By doing so, this work seeks to contribute new tools and methods for cell analysis and culture, that could pave the way for future advancements in biomedical research.

Chapter 2. Materials and methods

2.1 Materials and Reagents

Table 1. List of material and reagents of eDMA.

Name	Company	Country
Penicillin-Streptomycin(P/S)	Gibco Life Technologies GmbH	Darmstadt, Germany
Fetal bovine serum (FBS)	Gibco Life Technologies GmbH	Darmstadt, Germany
RPMI-1640	Gibco Life Technologies GmbH	Darmstadt, Germany
Modified Eagle Medium (DMEM)	Gibco Life Technologies GmbH	Darmstadt, Germany
Phosphate Buffered Saline (PBS)	Gibco Life Technologies GmbH	Darmstadt, Germany
Propidium Iodide (PI)	Invitrogen	California, USA
Hoechst 33342	Thermo Fisher Scientific Inc.	Massachusetts, USA
Calcein AM solution	Invitrogen (California, USA)	California, USA
0.25% trypsin/EDTA	Gibco Life Technologies GmbH	Darmstadt, Germany
Dimethyl sulfoxide (DMSO)	Sigma-Aldrich	St. Louis, Missouri, USA
Anti-Adherence Rinsing Solution	Stemcell Technologies Inc	Vancouver, Canada
3-D Life Dextran-PEG Hydrogel SG Kit	Cellendes	Kusterdingen,Germany
3-D Life Dextranase	Cellendes	Kusterdingen,Germany
Doxorubicin (DOX)	Sigma-Aldrich	St. Louis, Missouri, USA
HeLa CCL2	DSMZ GmbH	BraunschIig, Germany

SU-DHL4	DSMZ GmbH	BraunschIig, Germany
DMA slides	Aquarry	Karlsruhe,Germany
60-electrodes microelectrode arrays (60-MEA)	Centre for Biotechnology and Biomedicine of Leipzig University	Leipzig, Germany
Etoposide (ETO)	Selleckchem	Houston, Texas, USA

2.2 Design and fabrication of humidity chamber

The Electrode Droplet Microarray (eDMA) humidity chamber was designed using Rhino software. The Ultimaker 3 printer was set up, and PLA filament was selected as the material. The 3D model was loaded into the printer's software, the settings for PLA were adjusted, and the printing process commenced. Once printing was complete, the humidity chamber was removed from the printer, and any necessary post-processing steps were performed. Before conducting experiments on the eDMA, the humidity chamber was sterilized with 100% ethanol and air-dried under a laminar flow hood to ensure sterile conditions. Then, an appropriate amount of PBS and a moisture-absorbent pad were added to the humidity chamber to prevent droplet evaporation. The humidity chamber was placed in the incubator 10 minutes before performing any experiments.

The Droplet Microarray (DMA) humidity chamber was constructed using a petri dish, a moisture-absorbent pad was placed on the lid and saturated with 6-7 mL of PBS to maintain humidity, while an additional 2 mL of PBS was added to the bottom of the dish. This setup, with the DMA positioned within the petri dish, can prevent evaporation of the droplets, thereby preserving the microenvironment essential for cell culture experiments. The humidity chamber was placed in the incubator 10 minutes before performing any experiments.

2.3 Preparation of eDMA (electrode Droplet Microarray) slides

Hydrophilic-superhydrophobic patterned surfaces were acquired from Aquarray GmbH. Sixty-electrode microelectrode arrays (60-MEA) were manufactured by the Centre for Biotechnology and Biomedicine of Leipzig University. The method used for patterning MEA slides has been reported in previously published studies[44,145]. Here, I applied this method to the electrodes. The process began with the application of nanoparticle-poly layers to the MEA via a spin-coating technique. The creation of a superhydrophobic surface involved using a photomask to introduce fluorine groups under UV exposure. After removing the photomask, hydroxyl groups were added to make the surface hydrophilic, engineering 1 mm × 1 mm hydrophilic areas on the eDMA surface, each capable of accommodating three electrodes, as shown in Figure 8.

2.4 Water contact angle measurement

The eDMA surfaces have been prepared to ensure that they are clean and dry. Drops of 100 nL to 300 nL of deionized water were placed on the eDMA surfaces using a dispenser. The Krüss Drop Shape Analyzer machine from Hamburg, Germany, was then used to measure the water contact angles. The machine captured images of the water droplet on the surface and calculated the contact angle based on the shape of the droplet.

2.5 Cell culture

Culturing HeLa CCL2 cells. For culture HeLa CCL2 cells, the culture medium was prepared using Dulbecco's Modified Eagle Medium (DMEM) supplemented with 10% fetal bovine serum (FBS) and 1% Penicillin-Streptomycin (P/S). When thawing cells, frozen HeLa CCL2 cells were thawed in a water bath at 37°C, then transferred the cells to a 15

mL centrifuge tube. Prepared fresh culture medium in the centrifuge tube and ensured the water bath was heated to 37°C before the transfer. The cells were centrifuged for 3 minutes at 1200 RPM, the medium was discarded, and the cells were resuspended in the freshly prepared culture medium. An appropriate number of cells were seeded in culture dishes or flasks based on the desired confluence. The culture flask was placed in a 37°C incubator with 5% CO_2, allowing the cells to adhere and proliferate, changing the medium as needed. When the cells reached confluence, they were detached using trypsin-EDTA, neutralized with medium, and seeded in new flasks. The cells were regularly checked for confluence, morphology, and contamination, maintaining them in the logarithmic growth phase for experiments.

Culturing SU-DHL-4 cells. For culturing SU-DHL4 cells, the culture medium was prepared using RPMI-1640 medium supplemented with 10% FBS and 1% P/S. When thawing the cells, frozen SU-DHL4 cells were thawed in a water bath at 37°C, then transferred to a 15 mL centrifuge tube. Fresh culture medium was prepared in the centrifuge tube, ensuring the water bath was heated to 37°C before the transfer. The cells were centrifuged for 3 minutes at 1200 RPM, the medium was discarded, and the cells were resuspended in the freshly prepared culture medium. An appropriate number of cells were seeded in culture dishes or flasks based on the desired confluence. The culture flask was placed in a 37°C incubator with 5% CO_2, allowing the cells to proliferate. Once the cells reached confluence, they were transferred to a 15 mL centrifuge tube, centrifuged for 3 minutes at 1200 RPM, the old medium was discarded, and the cells were resuspended in fresh culture medium. An appropriate number of cells were seeded into new flasks. The cells were regularly checked for confluence, morphology, and contamination, maintaining them in the

logarithmic growth phase for experiments.

2.6 Cell culture on DMA and eDMA

Preparation of slides. The hydrophilic-superhydrophobic patterned surfaces from Aquarray GmbH. Then, DMA and eDMA were sterilized with 100% ethanol for 2 minutes and air drying under a laminar flow hood for at least 10 minutes to ensure sterile conditions. Prepared a humidity chamber following the previously described methodology.

Cell culture. For HeLa CCL2 and HEK 293T cells, DMEM supplemented with 10% FBS and 1% P/S was used. For SU-DHL4 cell RPMI-1640 medium supplemented with 10% FBS, and 1% P/S was used.

Printing of cells. The cells were washed by PBS. For adherent cells, the culture medium was removed from the flask using a suction pump to eliminate metabolic by-products and any non-adherent cells. The cell monolayer was washed twice with 5 mL of PBS, shaking the flask to ensure complete coverage and remove residual serum that inhibits trypsin activity. After the final PBS wash, the PBS was removed, and 1 mL of 37°C trypsin-EDTA solution was added evenly across the cell layer for uniform coverage. The flask was incubated at 37°C for 1 minute, observing the cells under a microscope to ensure they rounded up and detached without over-trypsinization. Following incubation, 5 mL of 37°C culture medium was added to neutralize the trypsin, using a pipet to create a single-cell suspension. The cell suspension was transferred to a 15 mL centrifuge tube and centrifuged for 3 minutes at 1200 RPM. For suspension cells, they were transferred to a 15 mL centrifuge tube and centrifuged for 3 minutes at 1200 RPM. After centrifugation, the supernatant of adherent and suspension cells was discarded without disturbing the cell pellet, and the cells were resuspended in 1 mL of fresh culture medium, pipetting to

achieve a homogeneous suspension. For the estimation of cell density, 10 µL of cell suspension was mixed with 10 µL of 0.4% Trypan Blue solution in a clean 1.5 mL Eppendorf tube, the stained cell suspension was loaded into a cell counting chamber using a pipette, and the chamber was placed in a Countess 3 automated cell counter. The cell suspension was dispensed onto the DMA and eDMA using an I-DOT One non-contact dispenser, printing 200 nL of the cell suspension. Afterward, the humidity chamber was attached to eDMA, or the DMA was placed into a humidity chamber using a petri dish to build a humidified environment.

Cell spheroids. To form spheroids from HEK 293T cells, before printing cells, 50 µL of the anti-adherence rinsing solution was mixed with 50 µL of DDH2O. Then, 50 nL was dispensed to each spot by an I-DOT One non-contact dispenser and dried under the hood. The printing step then followed. To establish a 3D cell culture on DMA utilizing the hanging drop technique as outlined in prior studies, the DMA slide was positioned on a designed polytetrafluoroethylene (PTFE) table[43]. A moisture-absorbent pad was placed in the Petri dish lid to mitigate evaporation during the culturing process, maintaining a consistent and conducive environment for the development of the 3D cell culture. To establish a 3D cell culture on eDMA, the slide was placed upside down using an adapter, and the eDMA and adapter were placed into a petri dish with a moisture-absorbent pad (10 mL PBS for the lid pad, 2 mL PBS for the petri dish) for 48 hours of culture in an incubator.

Culturing HeLa CCL2 cells in hydrogels on eDMA. To prepare the hydrogel precursor solution, distilled water, 10x concentrated Cell Buffer (CB) with a pH of 7.2, and SG-Polymer (such as Dextran) were combined in an Eppendorf tube, ensuring thorough mixing for a homogeneous solution. The desired cell suspension was incorporated, adjusting the cell

density as needed for the experiment, with 200 cells for HeLa CCL2 cells. Cross-linking agents (PEG-link) were introduced into the mixture to promote hydrogel formation. An I-DOT One non-contact dispenser was utilized to print 150 nL droplets of the cell-hydrogel suspension onto the DMA for microscopy-based analysis. The printed slide was placed into a humidity chamber to prevent droplet drying and incubated for at least 45 minutes to allow for full hydrogel formation. After the hydrogel had fully formed, each droplet was overlaid with 150 nL of cell culture medium and the slides were incubated in an impedance machine under the incubator for 24 hours.

Table 2. List of hydrogel precursor solution.

Reagents	Volumes for 100 µL gel (µL)
Water	35.3
10 x CB, pH 7.2	8
SG Dextran (30 mmol/L SH reactive groups)	6.7
Cell suspension	40
PEG-Link (20 mmol/L SH groups)	10
Total	100

2.7 Reusing of eDMA

Medium removal via HEMA-EDMA slide sandwiching was performed. A HEMA-EDMA slide was positioned on top of the eDMA and pressed to create a sandwich condition. This method absorbed and removed the cell culture medium from the hydrogel droplets without disturbing the

cells or the hydrogel structure. Then, 20 nL of 3-D Life Dextranase solution was dispensed onto each hydrogel spot containing the cell culture supernatant. The slides were incubated at 37°C for 40 minutes, allowing the Dextranase to enzymatically cleave the Dextran polymers within the hydrogel. The dissolution process was observed under a microscope to ensure complete degradation of the hydrogel matrix. The Phosphate-Buffered Saline (PBS) was used to wash the cells on the eDMA, applying the PBS to avoid dislodging or damaging the cells, while ensuring thorough removal of any residual hydrogel fragments or cellular debris. This washing step was crucial not only for cell recovery but also for the reuse of the eDMA slide, ensuring that no cells remained on the eDMA surface, and it could be reusable for future experiments.

2.8 Drug treatment on eDMA

The 1 mM Doxorubicin stock was used to obtain working solutions of 0.1, 0.5, 1, 5, and 10 µM by using cell culture medium. Then, using I-DOT One non-contact dispensing, 50 nL of each Doxorubicin solution was printed onto the droplets of eDMA. Following the dispensing of Doxorubicin solutions, the eDMA was placed in an impedance machine with a humidity chamber for real-time monitoring of cellular impedance for 48 hours.

2.9 Impedance spectroscope

The assessment of impedance spectroscopy utilized the MEA developed by the Centre for Biotechnology and Biomedicine at Leipzig University. These arrays were integrated with a multiplexer system 24, ensuring precise and multiplexed analysis of samples. For the impedance measurement, the impedance analyzer ISX-3, sourced from Sciospec Scientific Instruments in Germany, was employed. Raw data were

analyzed and processed with the self-developed software IDAT v3.6. The relative impedance (extracted cell signal) was calculated as follows. Relative impedance= ($|Z_{\text{with cells}}| - |Z_{\text{without cells}}|$) / $|Z_{\text{without cells}}| \times 100\%$.

2.10 Cell viability assay

The HeLa CCL2 and SU-DHL4 cells were cultured on eDMA as described above for 24 hours. Hoechst 33342, PI, and Calcein AM solutions were diluted with PBS to a final concentration of 5 μg/mL. The slides were incubated for 10 minutes at 37°C in the dark. Then, slides were placed on the stage of a fluorescence microscope. Images were captured using appropriate filter sets for Hoechst (excitation: 350-360 nm, emission: 460-470 nm), Calcein (excitation: 490 nm, emission: 515 nm), and PI (excitation: 535 nm, emission: 617 nm). The images were analyzed using ImageJ analysis software to quantify the number of live (Calcein AM-positive) and dead (PI-positive) cells. The cell images were imported into ImageJ, where they were manually counted using the multi-point tool. This process was done for each color of cell. The cell viability was calculated as follows. Cell viability%= alive cells (Calcein AM-positive)/total cells (Calcein AM-positive + PI-positive) ×100%.

2.11 Medium exchange on DMA

The HEMA-EDMA slide was sterilized using 100% alcohol and air-dried under a clean bench for approximately 10 minutes. The DMA slide with cells was fixed under the sandwiching adapter, with the HEMA-EDMA positioned above, forming a sandwich structure with the DMA slide and droplets in between. Pressing the HEMA-EDMA facilitated the transfer of culture medium from the DMA with cells to the HEMA-EDMA slide. Subsequently, the DMA was placed in a non-contact dispenser to add 150 nL of medium on top, everyday transferred medium once. This method

could effectively transfer half of the cell culture medium to the HEMA-EDMA slide.

2.12 Transfer cells to anther slide

The spheroids were cultured on one DMA slide for 48 hours using the previously described experimental approach. Another slide was seeded HeLa CCL2 cells for culture 48 hours. One DMA, which seeded HeLa CCL2 cells, was placed below the sandwich adapter, while the DMA, which seeded spheroids, was placed above so that the droplets from both DMAs came into contact. This arrangement facilitated the transfer of cells from the DMA on top to the one secured beneath the sandwiching adapter.

2.13 Lactate dehydrogenase (LDH) test

Table 3. List of LDH reaction mix.

Component	Reaction Mix(μL)
Developer Mix I/LDH Substrate Mix	2
PicoProbe III/Picoprobe	4
LDH Assay Buffer	89

Using a non-contact dispenser, 300 cells were seeded in 300 nL droplets across 672 spots on a DMA plate, with Etoposide added to achieve a final concentration of 20 μM. The plate was then placed in a humidity chamber and incubated for 48 hours. The experimental setup included negative controls (cells only), samples (cells with Etoposide treatment), a drug-only (20 μM Etoposide), only medium and positive control group, each with at least three replicates. After 48 hours, the LDH positive control was prepared and applied 300 nL to the DMA (100 μL culture medium + 2 μL LDH positive control solution). A new DMA was prepared for medium

transfer using the sandwiching method, followed by the addition of the LDH reaction mix, which was prepared in accordance with the specifications outlined in table 3. The humidity chamber petri dish was covered with foil and incubated for 5 minutes before imaging with a Keyence microscope to assess the results.

2.14 Statistical analysis

The experimental data in this research were based on at least 3 independent experiments. All impedance spectroscope data were analyzed by using software IDAT v4. The relative impedance was calculated as follows: Relative impedance= ($|Z_{\text{with cells}}| - |Z_{\text{without cells}}|$) / $|Z_{\text{without cells}}| \times 100\%$. The peak values (maximum amplitude) of the relative impedance, denoted as RI-Max%, percentage were then continuously monitored over time.

All data are presented as mean ± SEM. Experimental data were analyzed using unpaired t-tests for comparisons between two groups and one-way ANOVA for comparisons among three or more independent groups. Statistical significance in the t-test was assessed with a threshold of $P \leq 0.05$. Tukey's multiple comparisons test was performed following the one-way ANOVA to identify specific group differences, with significance indicated by $P \leq 0.05$. All statistical analyses were conducted using GraphPad Prism 8 (San Diego, CA).

Chapter 3 Results and discussion

3.1 Electrode Droplet Microarray(eDMA)

This chapter and related sections are under review in Advanced Healthcare Materials.

3.1.1 Fabrication of eDMA

The electrode Droplet Microarray (eDMA) slide was fabricated from four key components, as depicted in Figure 8a. These components include a glass substrate that serves as the foundational structure, a conductive pathway fabricated from gold due to its excellent electrical conductivity, a layer of SU-8 resist which adds structural integrity, and a precisely designed pattern of hydrophilic and hydrophobic regions, this pattern consistent with the descriptions provided in Figure 4.

Due to the manual nature of eDMA fabrication, there are slight differences in the dimensions of each eDMA slide. Figure 8b shows the specific dimensions of eDMA slide number 5808.

Each eDMA slide consists of an array of 5 × 4 hydrophilic spots, each measuring 1 mm by 1 mm, which covered three working electrodes (2 small electrodes. 0.4 mm × 0.1 mm and 1 big electrode. 0.4 mm × 0.15 mm). Together, the three electrodes formed three electrode pairs for the eDMA. L, R, W. I explored the impact of electrode pairs, I dispensed 200 nL of PBS on the eDMA spots and compared the impedance values of different electrode pairs. As expected, the impedance values obtained from the W electrode pair were significantly higher than those recorded from the L and R electrode pairs, 3686.9 Ω vs 2624.1 Ω, which is attributed to the fact that distance over which current passes through the pairs involving the W electrode is longer than that of the L and R.

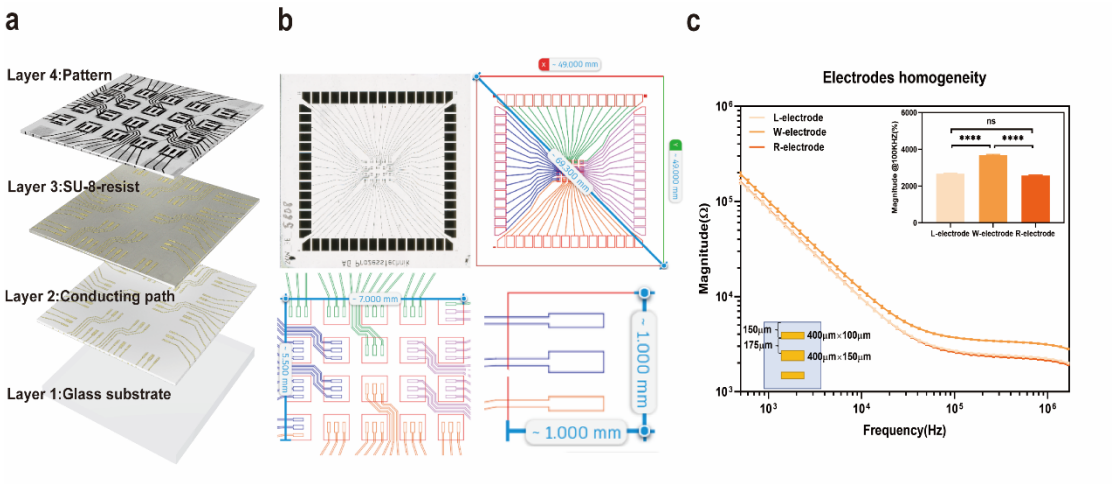

Figure 8. Fabrication of eDMA. a) The dimension of eDMA chip and hydrophilic-superhydrophobic array. As each DMA was made manually, each eDMA was assigned a unique serial number. b) Each eDMA is composed of 20 spots, each measuring 1 mm by 1 mm. On every spot, there are three electrodes, which come in two different sizes. c) Analysis of homogeneity of impedance signal obtained from different electrodes. Comparing the variability of impedance signal obtained from different electrode pairs. L-electrode pair, R-electrode pair, and W-electrode pair (n=20 electrodes, mean ± sem, * $P \leqslant 0.05$, ** $P \leqslant 0.01$, *** $P \leqslant 0.001$, **** $P \leqslant 0.0001$).

3.1.2 Droplet formation on eDMA

To evaluate the capability of the modified eDMA to support the formation of nanoscale droplets. Using a non-contact dispenser, I printed 200 nL of water onto the hydrophilic regions of the eDMA. As illustrated in Figures 9a, 9b, and 9c, this process resulted in the precise localization of droplets at the designated electrode sites.

Remarkably, each droplet, measuring 1 mm by 1 mm, was strategically positioned to enclose all three electrodes within its bounds (Figure 9c). This strategic placement enabled the formation of a 5 x 4 array of droplets, each precisely cover with the underlying 3 electrode architectures. The consistency and accuracy of droplet positioning emphasizes the ability of hydrophilic-hydrophobic patterns to ensure droplet formation and electrochemical analysis in specific areas of eDMA. Additionally, the eDMA platform can dispense 100 to 300 nL droplets using a non-contact dispenser due to the hydrophilic-superhydrophobic pattern (Figure 9d).

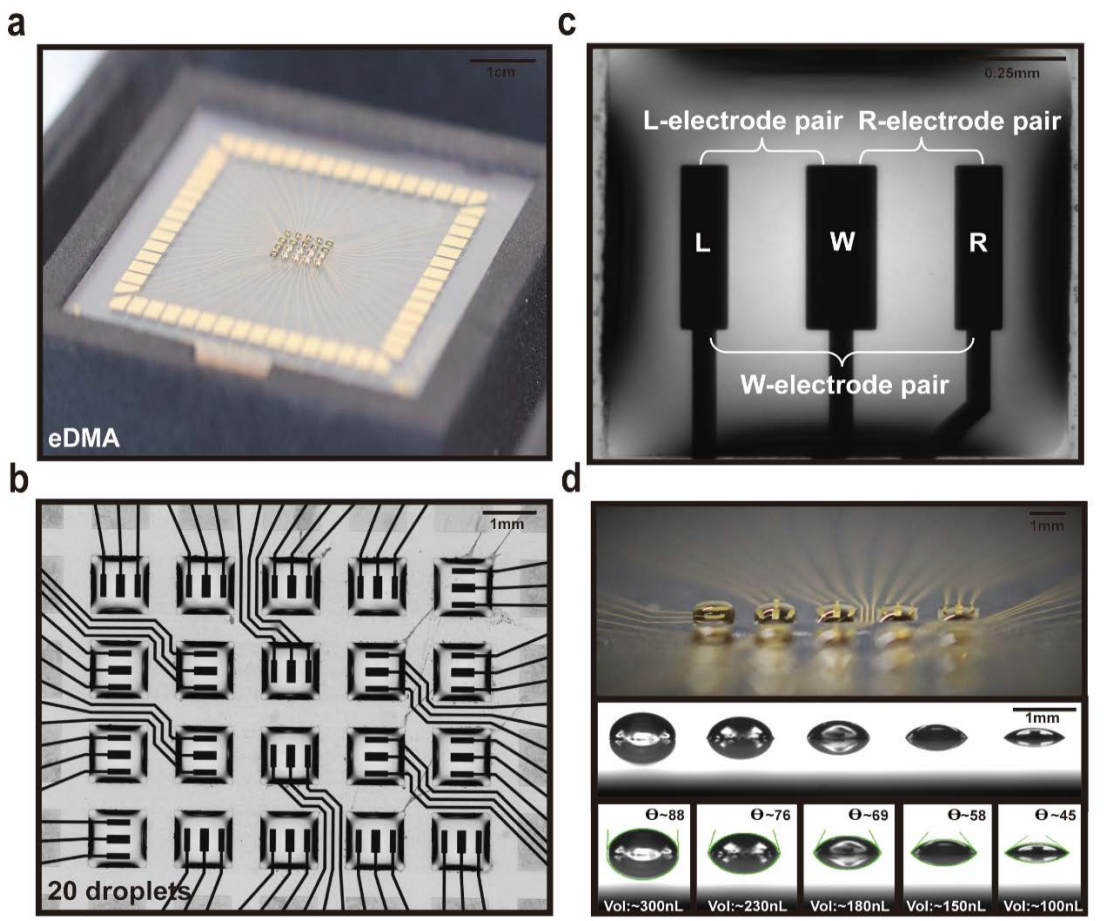

Figure 9. Droplet formation on eDMA. a) - b) Photographs of eDMA, showing the electrical circuit and the 5 × 4 array of 200 nL droplets formed on square 1 mm^2 hydrophilic spots each containing three gold electrodes. c) A photograph of a single 200 nL droplet on eDMA, containing three electrode pairs. L-electrode pair consisting of L and W electrode, R-electrode pair consisting of R and W electrode and W-electrode pair consisting of L and R electrodes. d) A photograph of the eDMA containing indicated volumes of water droplets. The lower panel shows the values of apparent water contact angle (θ).

3.1.3 Influence of coating on impedance measurement

Measuring impedance with eDMA differs from other state-of-the-art platforms in two ways. Firstly, it requires a specialized coating on the electrodes to create the hydrophilic-superhydrophobic pattern. Secondly, unlike standard microelectrode array (MEA) platforms, which employ microliter to milliliter volumes significantly larger than the electrodes, eDMA utilizes nanoliter droplets that are comparable in size to the single electrode. As a consequence, the small size and shape of the droplets can potentially affect the impedance measurements. To ensure the reliability and accuracy of impedance measurements using the eDMA system, I conducted validation of several parameters that could potentially influence measurement quality (Figure 10 and Figure 11).

First, the influence of the hydrophilic nanoparticle-based coating (coated eDMA) on impedance signal was investigated by measuring the impedance on coated and uncoated electrodes of different diameters, 50 µm, 100 µm and 200 µm, in 1 mL of cell culture medium (Figure 10a and d-f). The results revealed that at low frequencies, coated eDMA showed an increase in impedance magnitude compared to uncoated eDMA, while no significant difference was observed at higher frequencies (Figure 10a).

The equivalent circuit model (ECM) consists of a constant phase element (CPE_{el}) that reflects the non-ideal capacitive characteristics, in series with the spreading resistance (R_S) observed across the electrode-electrolyte interface (Figure 10b). The ECM-derived impedance spectra fitting graph was created by our collaborative research group. ECM derived impedance spectra fitting fits quite well to the measured impedance magnitude and phase angle of electrodes without cells (Figure 10c). Based on the ECM fittings, they statistically analyzed the values of CPE_A, CPE_n and R_s (Figure 10g-i). The constant phase element CPE_{el} describes the non-

ideal capacitance of the electrical double layer at the electrode-electrolyte interface with the parameter CPE_A (capacitance) and CPE_n that describes how closely the CPE behavior approximates an ideal capacitor. Such capacitors do not exist in real life. Values of CPE_n close to 1 indicate nearly ideal capacitive behavior of electrode, while values less than 1 indicate increasing deviation from ideal behavior due to e.g. surface roughness or inconsistencies. Our results show that coated electrodes have significantly lower $CPE_{A,}$ $2.782*10^{-8}$ F vs. $6.093*10^{-9}$ F, but higher $CPE_{n,}$ 0.8509 vs. 0.9514. Lower CPE_A indicates that the coated electrode reduces its effective capacitance, which could mean that the coating modifies the electrode's surface properties. Higher CPE_n however demonstrates that the hydrophilic coating results in electrodes being closer to ideal capacitance in comparison with uncoated electrodes (Figure 10g, h). All together this indicates that the coating leads to a more uniform and less obstructive surface, allowing for a more ideal capacitive behavior. R_s represents the real impedance encountered as electrical current moves from the boundaries of the electrode surface through the electrolyte. The obtained values of R_s from coated versus uncoated electrodes revealed no significant differences (Figure 10i). Thus analysis results suggest that while the hydrophilic coating modifies the capacitive properties of the electrodes, however without substantially affect their ability to conduct current, hence maintaining the integrity of impedance measurements.

Next, to examine whether a hydrophilic coating affects the monitoring of cell growth via impedance spectroscopy. Human Embryonic Kidney 293A cells (HEK293A) were seeded onto circular electrodes (50 µm, 100 µm, 200 µm) and cultured in a cell incubator for durations of 24, 48, 72, and 90 hours, as shown in Figure 10d-f. Then relative impedance maximum (RI-Max%) of cells cultured on coated versus uncoated

electrodes was compared. RI-Max% is an impedance measured at a single frequency, at which given cells show maximum impedance signal, and since it is relative, normalized against a control, it reflects the difference between cells on coated versus uncoated electrodes. Results revealed generally lower signals from the coated electrodes across all sizes and times. However, the growth trends observed by impedance spectroscopy were similar for both electrode types, suggesting that despite the slightly lower impedance signals from coated electrodes, the hydrophilic coating does not significantly interfere with the ability to monitor cell growth through impedance measurements. This confirms the compatibility of the coating with impedance-based cell growth monitoring.

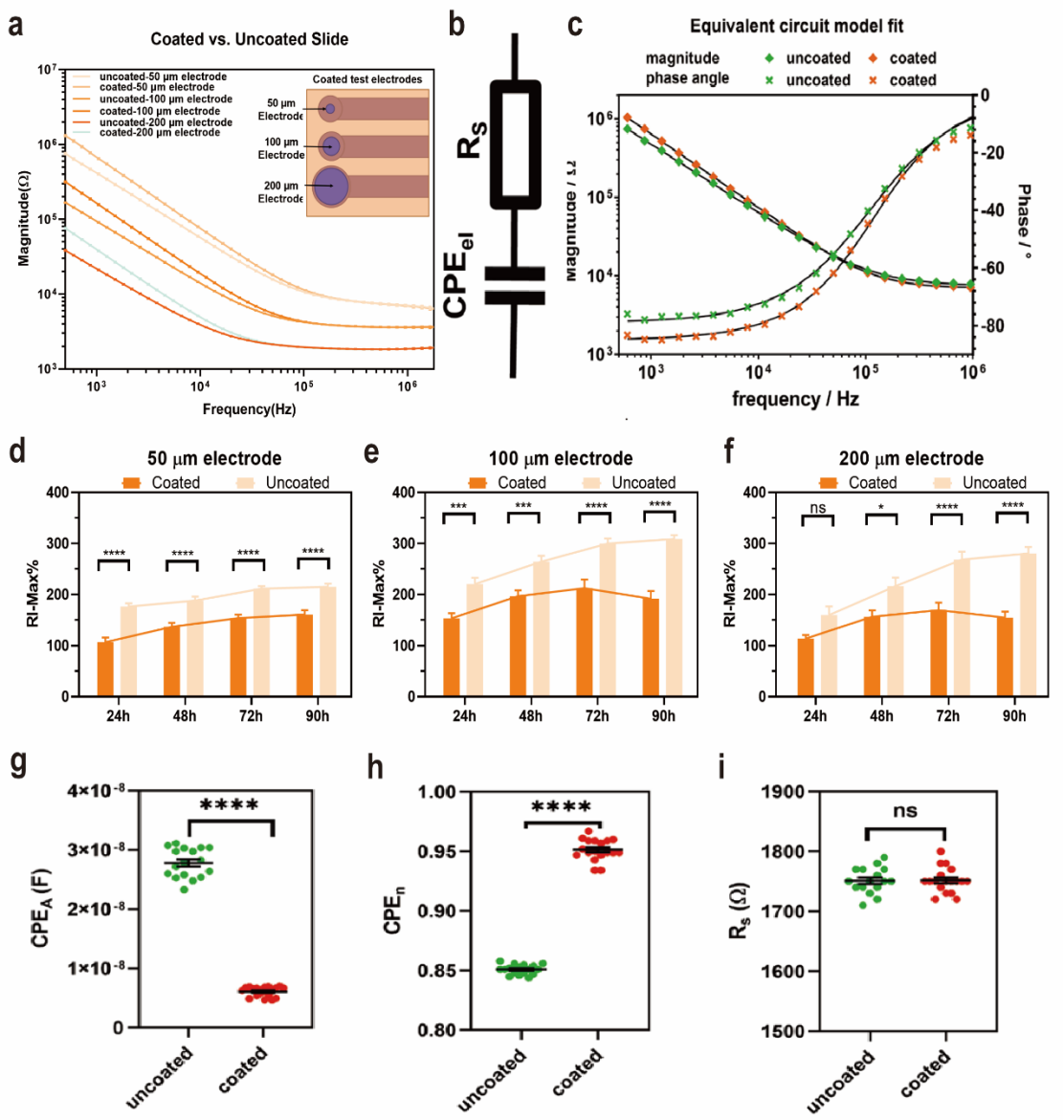

Figure 10. Influence of coating on impedance measurement. a) Comparison of the measurements of impedance conducted on round electrodes with diameters of 50 µm, 100 µm, and 200 µm, both uncoated and coated with a hydrophilic coating, within a 1 mL medium. The variation in impedance magnitude among electrodes, wherein impedance decreases with increasing electrode size, can be attributed to the larger surface area of the bigger electrodes. This increased surface area can accommodate a greater number of charge carriers, thereby reducing resistance to the flow of electrical current and resulting in decreased

impedance (n=15 electrodes). b) Equivalent circuit model (ECM) for electrode-electrolyte interface. c) Comparison of measured impedance magnitude and phase angle spectra (symbols) and ECM-fitting derived spectra (black lines). d) - f) RI-Max% measurements of HEK293 cells cultured on coated and uncoated round electrodes with diameters of 50 µm, 100 µm, and 200 µm for 90 hours (n=12 electrodes). g) - i) Analysis of ECM parameter for capacitance (CPEA, n) and resistance (RS) (n=18, mean ± sem, * P ⩽ 0.05, ** P ⩽ 0.01, *** P ⩽ 0.001, **** P ⩽ 0.0001).

3.1.4 Influence of droplet curvature and volume on impedance measurement

The standard droplet volume for cell culture application on the DMA platform is 200 nL confined on a 1 mm² square area, the height of such droplet in the middle is about 0.3 mm, which is comparable with the size of the electrodes. Such small liquid layer over the electrodes is not common in standard MEA measurements and can influence the impedance measurement of the electrodes. To investigate the influence of different volumes on impedance measurements, our collaborative group first employed finite element method (FEM) simulations to model signal outputs from droplets of various volumes, aligning this theoretical framework with experimental data, as demonstrated in Figure 11.

FEM allowed us to anticipate the behavior of different volume droplets, providing a theoretical framework to compare against experimental data. The calculated electric potentials demonstrate that as droplet volume decreases (from 300 nL to 25 nL), the potential difference notably increases, with the potential increasing at the edges near the electrodes and decreasing in the middle. This gradient in potential difference is more pronounced in smaller droplets due to the edges being

in closer proximity to the electrodes. These results indicated that, with decreased droplet volumes, the distribution of the electric field within the droplet becomes increasingly inhomogeneous, concentrating the field strength at the periphery while weakening it at the center. This uneven electric field distribution can negatively affect impedance measurements. The simulation results showed that the current was slightly concentrated at the edge of the electrode. As the droplet volume decreases, the current density at the electrode-droplet interface increases significantly, the current density at the edge electrode increases significantly, which means current was unevenly distributed on the electrodes in smaller droplets. All together, these suggest that smaller droplet volumes focus electric fields and current density at their interfaces, potentially affecting impedance measurements due to the non-uniform distribution of current (Figure 11a).

Then, the FEM simulation model was used to calculate impedance magnitude and phase angle spectra, which fitted nicely with experimental measured impedance spectra (Figure 11b). The simulation derived impedance magnitude spectra for droplets ranging from volumes of 12.5 nL to 350 nL showed no significant increase of impedance between volumes of 150 and 300 nL (Figure 11c). A comparison of experimental measurements and simulation data at 100 KHz using all three electrode pairs showed good concordance across all volumes (Figure 11d and 11e), confirming that measurement in droplets above 150 nL are reliable, and volume variations between 150 and 350 nL do not adversely affect the measurements. I have also assessed consistency and reliability of measured signal for repeated use of eDMAs (Figure 11f). The findings revealed no significant variance in impedance values between different time points, underscoring the robustness of measurements on eDMA platform.

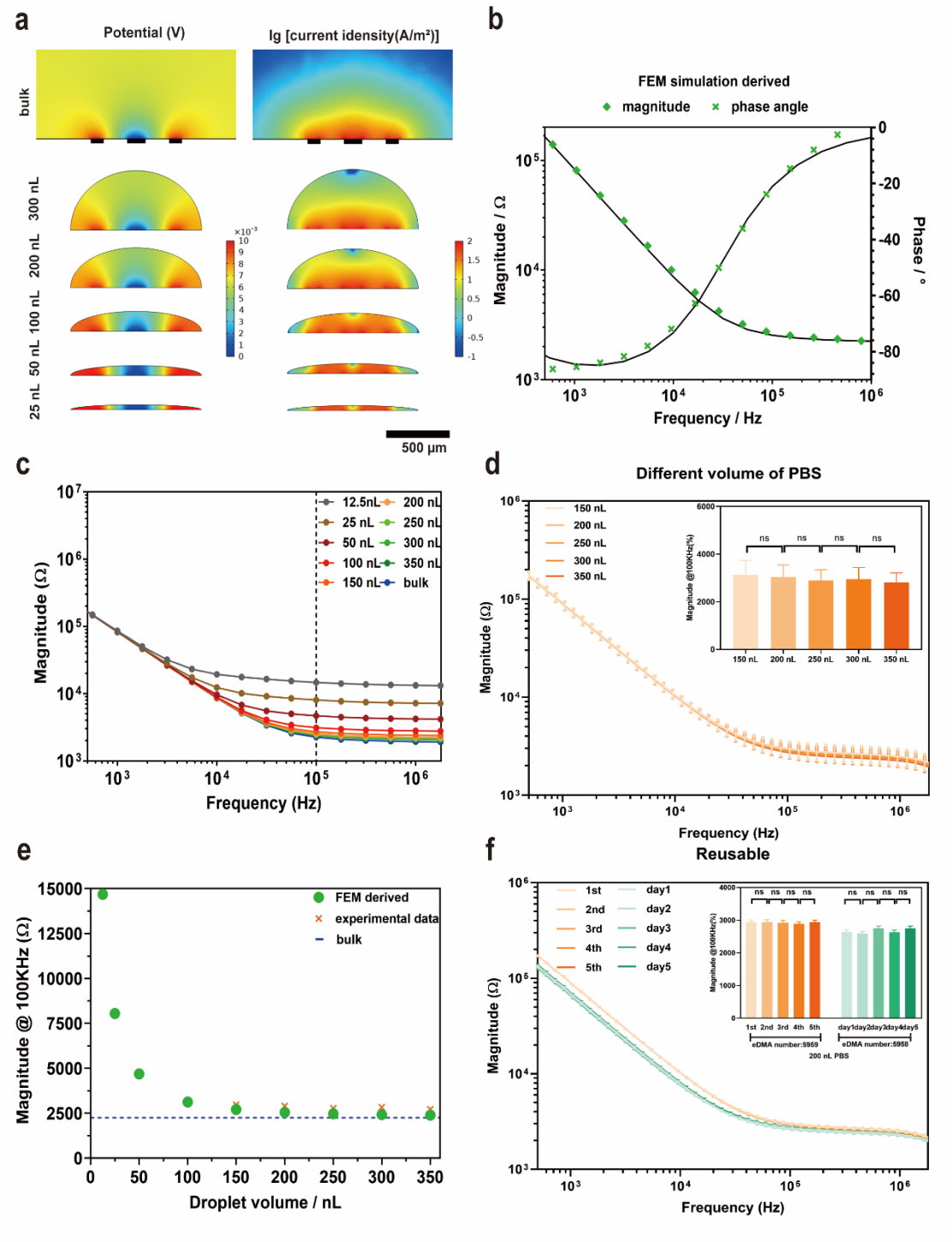

Figure 11. Influence of droplet curvature and volume on impedance measurement. a) FEM simulation model derived potential and current density for different droplet volumes. b) Comparison of FEM simulation derived impedance magnitude and phase angle spectra (black lines) and experimentally measured spectra (symbols). c) The impedance magnitude

spectra derived from FEM simulation model corresponding to droplets of different volumes ranging from 12.5 to 350 nL. d) Examining variations in the impedance magnitude in different droplet volumes on eDMA (n=39 electrodes). e) Comparison of impedance magnitudes obtained experimentally at 100 KHz in droplets of different volumes and in FEM simulation. (green symbols for FEM derived results; red symbols for experimental results; blue line for bulk). f) Investigation of the reusability of eDMA. The impedance measurements were conducted in 200 nL of PBS within a single day and over several days to evaluate the consistent performance of eDMA over time (n=58 electrodes for eDMA 5959; n=50 electrodes for eDMA 5958). (mean ± sem, * $P \leqslant 0.05$, ** $P \leqslant 0.01$, *** $P \leqslant 0.001$, **** $P \leqslant 0.0001$).

3.1.5 Adherent cell culture on eDMA

To validate the efficacy of the eDMA platform for supporting the cultivation of adherent cells, I selected HeLa CCL2 cells as a model system. A precise quantity of 300 HeLa CCL2 cells, suspended in 200nL droplets, was carefully dispensed onto both traditional Droplet Microarray (DMA) and the enhanced eDMA surfaces. Following a 24-hour incubation period, cell viability was meticulously assessed through microscopy. It was observed that the HeLa CCL2 cells successfully formed a monolayer on both the DMA and eDMA surfaces after the incubation, with no significant disparity in cell viability between the two platforms, as illustrated in Figures 12a, b. These findings underscore the eDMA's capability to provide an optimal environment conducive to cell growth, thereby affirming its suitability for cell culture applications.

To further uncover the complex dynamic relationship between cell density and the resulting relative impedance measurements, I started on following study. This involved dispensing different number of cell populations, ranging from 200 to 1000 cells, into 200 nL droplet on the eDMA chips. Following a 24-hour period, which allow the HeLa CCL2 cells to form monolayer, I proceeded to monitor the impedance signals over 2 hours. The analysis results showed that positive correlation between an increase in cell number and a corresponding increase in relative impedance values, as shown in Figure 12c. This result emphasizes the premise that in the case of adherent cells, relative impedance can as a reliable indicator of cell density.

Taken together, these investigations not only validate the eDMA platform's efficacy in adherent cell cultures but also its ability to precisely quantify cell proliferation through impedance measurements.

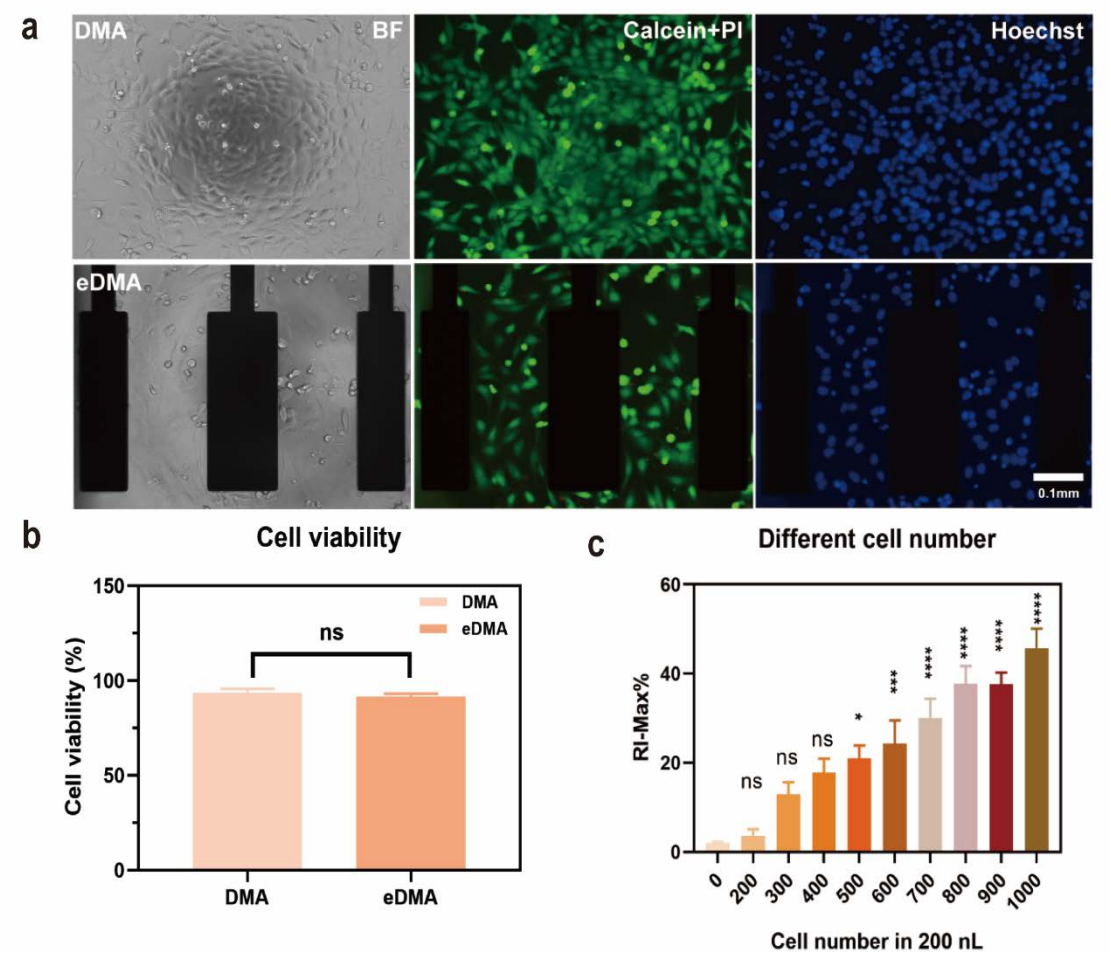

Figure 12. Adherent cell culture on eDMA. a) Compare image of HeLa CCL2 cells on DMA and eDMA after 24 hours culture. $1.5*10^6$ /mL HeLa CCL2 cells were seeded on DMA and eDMA for 24 hours culture in the incubator. HeLa CCL2 cells can form monolayer on DMA and eDMA after 24 hours cell culture in incubator. b) Comparison of HeLa CCL2 cell viability on DMA and eDMA. HeLa CCL2 cell viability was analyzed by using 5 µg/mL Hoechst, Calcein AM and PI after 24 hours culture. c) After 24 hours HeLa CCL2 cell culture, impedance on 24th hour be given a compare with different cell numbers. All of different cell numbers are compared to 0 cells to make significant differences. (Blue. Hoechst; Green. Calcein AM; Red. PI) (* $P \leqslant 0.05$, ** $P \leqslant 0.01$, *** $P \leqslant 0.001$, **** $P \leqslant 0.0001$).

3.1.6 Suspension cell culture on eDMA

To evaluate the eDMA platform's capacity to culture suspension cell types, the SU-DHL4 cell line was selected as a representative model for this study. I used 300 cells of SU-DHL4 cells in 200 nL volume, printed into the surfaces of both the DMA and the eDMA. After a 24-hour incubation period, helping cell adaptation and potential proliferation, cell viability was extensively assessed using microscopy techniques. The analysis revealed that the SU-DHL4 cells exhibited high viability on both platforms, with no significant differences in cell survival rates between the DMA and eDMA, as shown in Figures 13a and b. This outcome demonstrates the eDMA's have ability to create an ideal microenvironment that suspension cell growth.

To gain insight into the dynamics of interactions between suspended cells and electrodes, I dispensed a range of cell numbers (ranging from 200 to 1000 cells) onto the eDMA chip, each within a precisely measured 200 nL droplet. Impedance measurements were taken immediately afterwards to capture any immediate changes in electrical characteristics. Interestingly, the analysis revealed that the lack of significant correlation between relative impedance values and suspended cell density, a phenomenon documented in detail in Figures 13c. This unexpected result indicated at potential limitations in the sensitivity of current eDMA system, specifically their ability to distinguish and accurately reflect impedance changes induced by suspended cells.

This finding not only reveals the complexity of cell-electrode interactions in eDMA settings but also highlights the need for further refinement of eDMA technology.

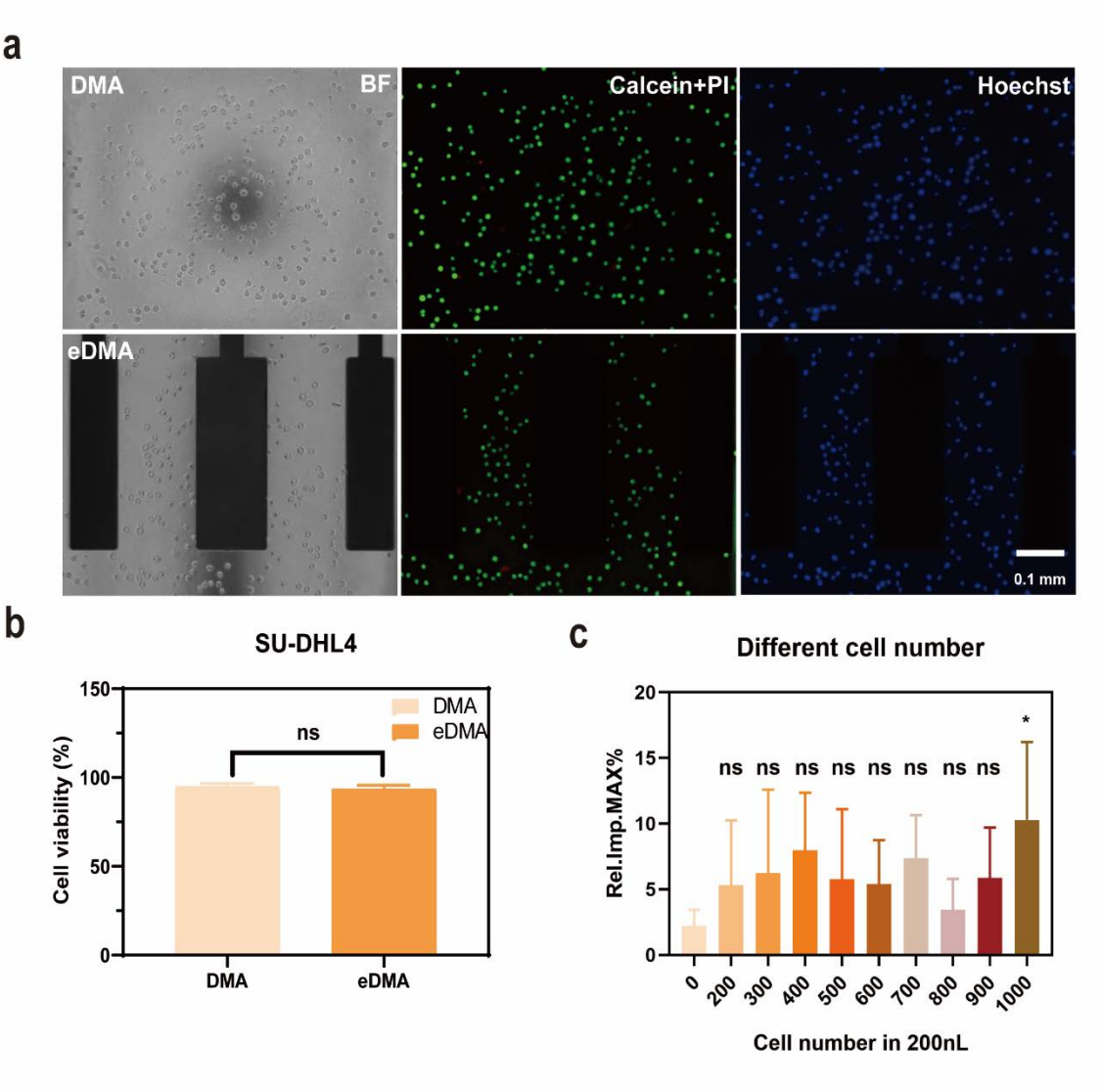

Figure 13. Suspension cell culture on eDMA. a) Compare image of SU-DHL4 cells on DMA and eDMA after 24 hours culture. 1.5*10^6/mL SU-DHL4 cells were seeded on DMA and eDMA. b) Comparison of SU-DHL4 cell viability on DMA and eDMA. SU-DHL4 cell viability was analyzed by using 5 μg/mL Hoechst, Calcein AM and PI. c) Impedance be given a compare with different cell numbers. All different cell numbers are compared to 0 cells to make significant differences. (Blue. Hoechst; Green. Calcein AM; Red. PI) (* P ⩽ 0.05, ** P ⩽ 0.01, *** P ⩽ 0.001, **** P ⩽ 0.0001).

3.1.7 Cell spheroids culture on eDMA

To investigate the potential impact of cell spheroids on impedance values, I initiated an experiment by seeding a range of 300 - 600 cells in 200 nL droplets onto the eDMA platform. Following 48 hours of incubation, the cells were expected to aggregate into spheroids. Subsequently, the eDMA was placed into an impedance measuring device, where impedance readings were taken over 2 hours to facilitate a comparative analysis of the impedance data.

To promote the formation of cell spheroids and minimize cell adhesion, I initially applied an anti-cell adhesion coating onto the eDMA surface. This was achieved by printing 50 nL of the coating solution onto the eDMA and allowing it to air-dry under a hood, thereby creating a less adhesive environment conducive to spheroid formation. To determine whether this coating would influence impedance measurements, I conducted a comparison between coated and uncoated eDMA platforms. The findings indicated that the presence of the coating did not significantly affect the impedance values (Fig14 a).

In subsequent experiments, the eDMA was coated before seeding different concentrations of HEK 293T cells. After 48 hours of inverted culture within the incubator through a humidity environment built by petri dish, impedance measurements were conducted in both straight and upside-down positions over a 2-hour period. The method was designed to determine whether the orientation during the measurement results in any changes in impedance, particularly as HEK 293T cells tend to form spheroids when cultured in upside-down droplets. The comparative analysis of these two measurement methods revealed no significant changes in impedance values across various cell densities forming spheroids, regardless of the measurement orientation (Fig14 b-c). This

outcome suggests that the eDMA platform may not be ideally suited for the culture of cell spheroids, as the formation of spheroids did not significantly influence the impedance readings, indicating a potential limitation of the eDMA in capturing the unique electrical properties associated with spheroid cellular structures.

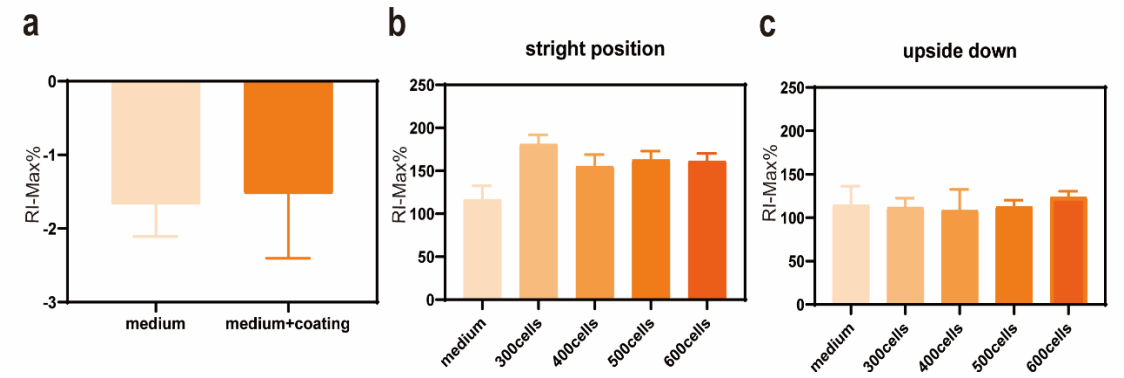

Figure 14. Cell spheroids culture on eDMA. a) Compare RI-Max% of with anti-cell adhesion coating and without anti-cell adhesion coating. b) - c) Different concentration of HEK 293T cells were seeded on eDMA, after 48 hours upside-down culture under incubator, impedance was recorded 2 hours by using straight position recoding and upside-down position recoding.

3.1.8 Cell culture in hydrogels

To evaluate the suitability of the eDMA platform for three-dimensional (3D) cell culture, I cultured cells in a hydrogel matrix to examine the resulting impedance changes. The results shown in Figures 15a and b indicate that there are no significant changes in impedance values. This leads to the conclusion that the eDMA platform may not be ideally suited for 3D cell culture applications, as the incorporation of cells into a 3D hydrogel environment did not induce detectable impedance changes.

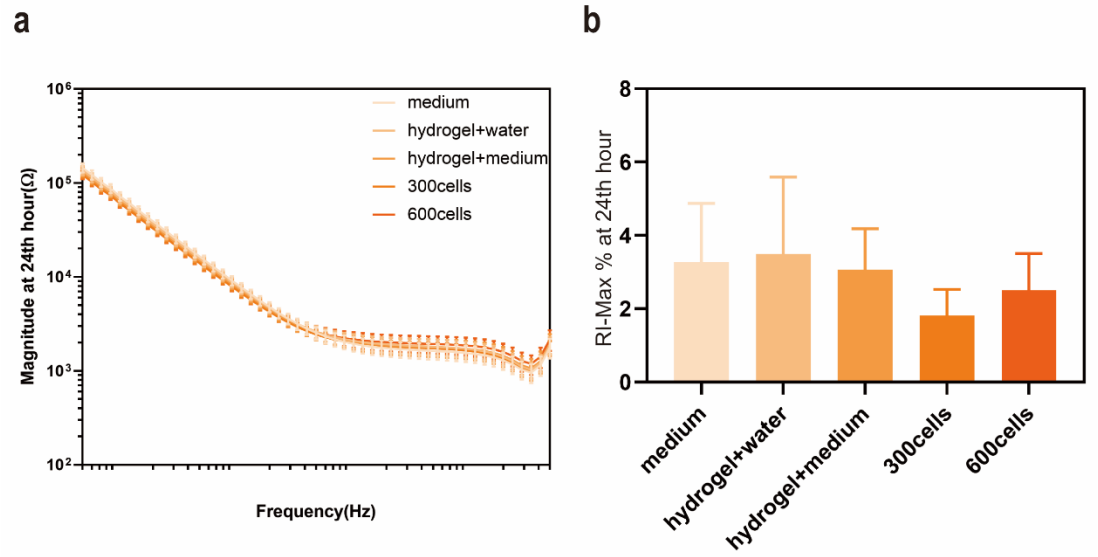

Figure 15. Cell culture on hydrogel. a) Compare impedance. medium, hydrogel + water, hydrogel + medium, 300 cells culture on hydrogel, 600cells culture on hydrogel after 24 hours culture. b) Comparison of RI-Max% at 24th hour.

3.1.9 Humidity chamber of eDMA

In experimental setup, the Ultimaker 3 printer was employed, utilizing PLA ink to fabricate a humidity chamber, the dimensions of both the chamber and its lid are shown in Figures 16a and b. Figure 16c shows the assembly after the humidity chamber has been secured to the eDMA using double-sided tape, ensuring a secure and airtight seal.

To evaluate the efficacy of the chamber in avoiding evaporation, I added 200 nL of cell culture medium onto the eDMA and sticked humidity chamber immediately, then did a continuous monitoring over 48 hours. Comparative analyses were conducted at the start time (0 hours), middle time (24 hours), and end time (48 hours) of this period. As shown in Figure 16d, the results revealed no significant fluctuations in impedance values across various frequencies.

Then I compared the impedance magnitudes at a frequency of 100 KHz. The results, illustrated in Figure 16e, indicate no significant difference in impedance values at the 0, 24, and 48-hour. Furthermore, a comparative visual analysis between the images captured at 0 hours and at 48 hours revealed no significant differences, confirming the visual consistency of the eDMA surface over the duration of monitoring. This consistency highlights the ability of our humidity chambers to maintain a stable humidity environment on eDMA for at least 48 hours. This finding is critical because it validated the role of the humidity chamber in maintaining an optimal microenvironment for cell studies on the eDMA platform, thereby increasing the reliability and reproducibility of our experimental results.

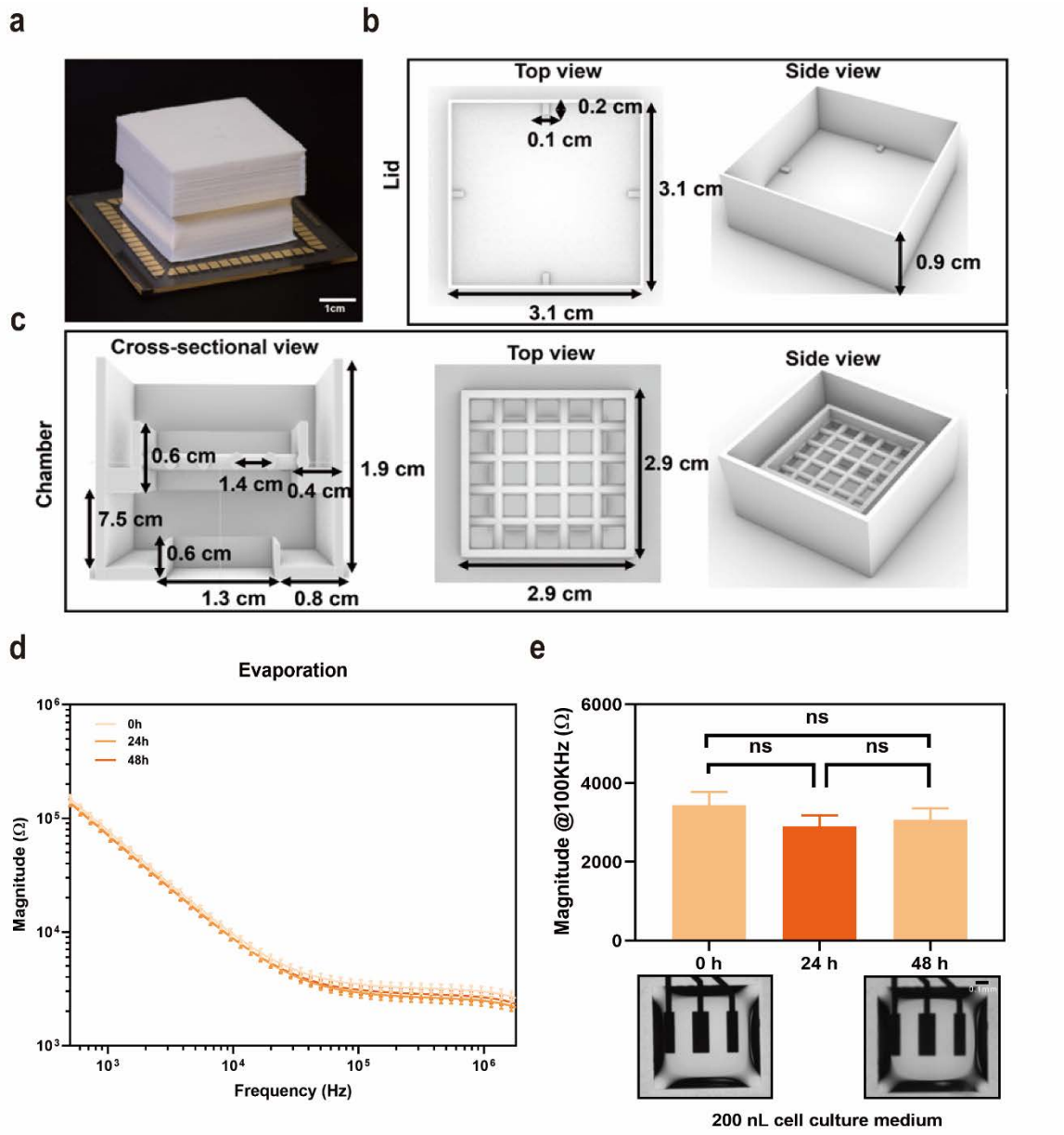

Figure 16. Humidity chamber of eDMA. a) A photo of humidity chamber attached to eDMA. b) The design of humidity chamber lid. Tissue pad was placed inside the lid and wetted with 1 mL PBS. c) The design of humidity chamber. 2 mL of PBS was filled in all channels in the chamber. d) - e) Impedance measurements obtained from 200 nL droplets of cell culture medium on eDMA at 0, 24 and 48 hours, and corresponding microscope images of the droplets, demonstrating the possibility of continuous monitoring of stabile impedance signal on the eDMA platform for 48 hours

(n=3 electrodes). (mean ± sem, * P ⩽ 0.05, ** P ⩽ 0.01, *** P ⩽ 0.001, **** P ⩽ 0.0001)

3.1.10 Real-time monitoring of cells and characterization of cells

I wanted to verify that the experimental conditions provided by the humidity chamber are optimal for preserving cell health and accurately capturing impedance changes, I conducted assessment of cell compatibility within this controlled environment by real-time recording impedance spectroscopy on HeLa CCL2 cells for 24 hours (Figure 17). I used a non-contact dispenser to seed $3*10^6$ /mL HeLa CCL2 cells in eDMA, which were then immediately placed into the impedance measuring device for real-time monitoring for 24 hours.

I tracked the graphical representation of the maximum impedance over time, I observed a rapid increase in the first 4 hours of culture, probably reflecting the initial settling and adhesion of cells onto the electrode's surface; between 4 and 15 hours, RI-Max% was continuously increasing due to cell proliferation; after 15 hours the growth of cells slow down with the curve showing stable cell monolayer with slight decrease towards the 24 hours point. As a result, I successfully demonstrated the continuous monitoring of cell culture on eDMA for a 24-hour period utilizing impedance spectroscopy (Figure 17a, b). After 24 hours of real-time monitoring, the cells continued to grow effectively on the electrode surface of the eDMA. The images demonstrate that the cells are firmly attached to the electrodes (Figure 17c). All of results suggest a significant impact of cellular attachment and growth on the electrodes of eDMA.

This detailed analysis not only confirms the ability of eDMA to support cell growth but also elucidates the dynamic impact of cellular

processes on impedance measurements, providing valuable insights into the integration of biological systems with electrochemical sensing technologies.

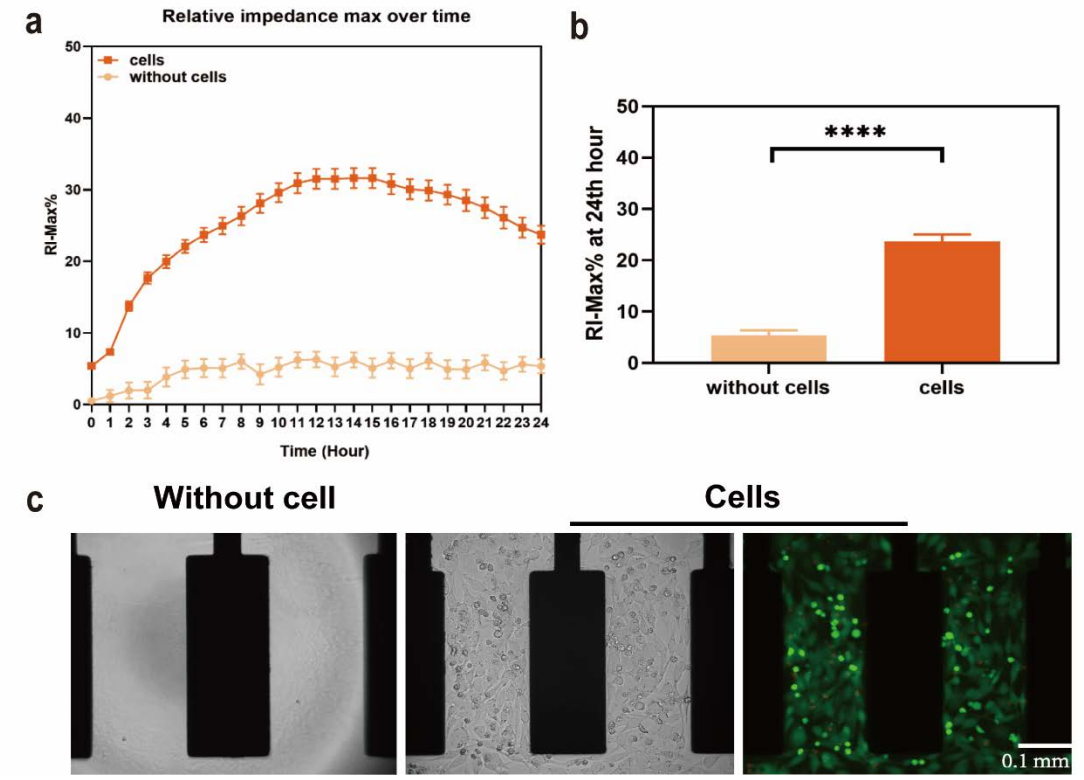

Figure 17. Real-time monitoring of cells and characterization of cells. a) Continuous monitoring of RI-Max% of cells versus empty droplets over 24 hours of culture. b) Extracted values of RI-Max% obtained from droplets with cells and cell culture medium at 24 hours of culture. c) Compare image of eDMA without cells and with cells after 24 hours culture. (n=23 electrodes for cells, n=7 electrodes for without cells, mean ± sem, * $P \leqslant 0.05$, ** $P \leqslant 0.01$, *** $P \leqslant 0.001$, **** $P \leqslant 0.0001$).

3.1.11 Drug-treatment on eDMA

I further performed treatment of HeLa cells with Doxorubicin (DOX) and compared dose-response of HeLa cells culture on eDMA (Figure 18). HeLa CCL2 cells were seeded 600 cells per 200 nL ($3*10^6$ /mL) by using non-contact dispenser and incubated overnight until form cell monolayer. Afterwards, HeLa CCL2 cells were treated with DOX for 24 hours by adding 50 nL DOX that was diluted with culture medium till desired concentrations (0.1 µM, 0.5 µM, 1 µM, 5 µM, 10 µM) and real-time recorded impedance spectroscopy for 48 hours. Then for visualization of cell viability, HeLa cells were stained with Calcein AM and Propidium iodide (PI) for 15 mins.

I observed that it is possible can real-time monitoring drug-response for 48 hours and relative impedance MAX%(RI-Max%) decrease with DOX concentration increase. During the 48-hour impedance monitoring, a steady rise in impedance was noted when DMSO was used in the initial 24 hours. After 24 hours, a slight decline in the RI-Max% was observed, likely due to the cells reaching confluence on the droplet, causing there is no nutrients to provide cells with growth. However, as the concentration of DOX increased, especially with high concentrations of 1 µM, 5 µM and 10 µM stimulating the cells, there was a decrease in RI-Max% over time, particularly during the 24-hour to 48-hour (Figure 18a and Table 4).

To further elucidate the dose-dependent effects of drugs, I evaluated of IC50 values using relative impedance. The method for calculating IC50 based on impedance involved normalizing the RI-Max% values for each concentration of DOX treatment relative to the RI-Max% of DMSO at each time point during 48h of drug treatment. Through the eDMA platform, cell response to DOX for 48 hours was quantitatively analyzed, this data enabled the calculation of IC50 values, which decreased from 10.48 µM

(95% confidence interval (CI_{95}) 7.40-15.21 µM) at 24 hours to 5.63 µM (CI_{95} 4.12-7.72 µM) at 48 hours, indicating an enhanced drug sensitivity over time. Additionally, cell viability was assessed using Calcein AM and PI staining, IC_{50} derived from microscopy-based read-out are 3.86 µM (CI_{95} 2.79-5.31 µM) at 24 hours and 1.87 µM (CI_{95} 1.22-2.85 µM) at 48 hours, which provided a basis for further IC50 determinizes, highlighting the dynamic responses of cells to DOX treatment over time. (Figure 18b and c). Overall, the determined IC50 values of both methods are in the same range, whereas microscopic determined IC50 values in general with no significant difference for 48 hours but for 24 hours. This suggests that the eDMA platform aligns more closely with traditional microscopy at later time point. This is due to the limitations of endpoint methods such as microscopy, which do not provide insights into intermediate points.

I used a consistent approach to calculate IC50 values at 6-hour intervals using maximum relative impedance data, applying sigmoidal fitting for time analysis (Figure 18d). I demonstrated the possibility to extract the information about the drug response at any time of experiment, which is not possible with endpoint assays as live/dead staining and microscopy (Figure 18d).

In conclusion, our findings underscore the eDMA platform's efficiency in real-time label-free and non-invasive monitoring of cell drug responses within a nanoliter format.

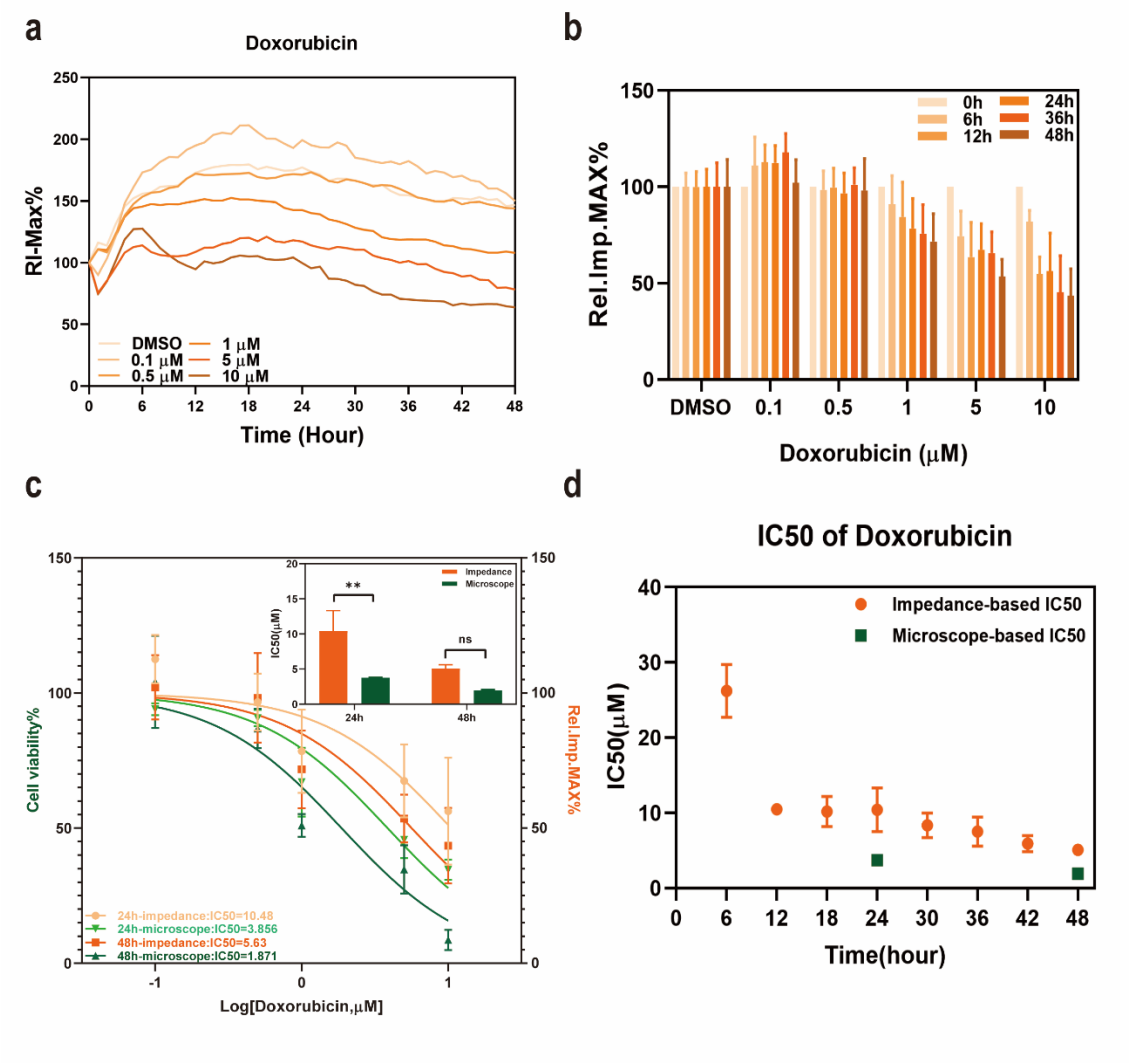

Figure 18. Real-time monitoring drug response of cells on eDMA. a) Continuous RI-Max% measurements from HeLa CLL2 cells treated with different concentrations of DOX over 48 hours. b) Extracted values of RI-Max% at 6 h, 12 h, 24 h, 36 h and 48 h for different concentrations of DOX and vehicle control. Significance indicates the comparison of each time point within the concentration groups to time zero. c) Concentration-dependent curves and calculated IC50 values using EIS and microscopy at 24 and 48 hours of incubation. Impedance based IC50 value at 24 hours was 10.48 µM with 95% confidence interval between 7.40 and 15.21 µM; and at 48 hours - 5.63 µM with 95% confidence interval between 4.12 and 7.72 µM. Microscope based IC50 value at 24 hours was 3.86 µM with 95%

confidence interval between 2.79 and 5.31 µM; and at 48 hours - 1.87 µM with 95% confidence interval between 1.23 and 2.85 µM. d) Estimated IC50 values at 6-hour interval using EIS in comparison with IC50 values at 24 and 48 hours using microscopy. DMSO. n=10; 0.1 µM. n=6; 0.5 µM and 5 µM. n=7; 1 µM. n=12; 10 µM. n=9 electrodes. Microscopy. n=3 (mean ± sem, * P ⩽ 0.05, ** P ⩽ 0.01, *** P ⩽ 0.001, **** P ⩽ 0.0001).

Table 4. Statistical analysis for relative impedance of Doxorubicin-cell response (Figure 18b) (DMSO. n=10; 0.1 µM. n=6; 0.5 µM and 5 µM. n=7; 1 µM. n=12; 10 µM. n=9 electrodes).

	RI-Max% (mean ± sem)					
Hour	DMSO	0.1 [µM]	0.5 [µM]	1 [µM]	5 [µM]	10 [µM]
1	116.3±5.9	203.6±3.6	110.8±3.2	110.9±4.6	75.5±7.1	74.6±11.3
2	113.9±4.3	205.4±4.1	108.3±2.3	110.2±3.9	85.3±1.7	84.8±5.1
3	131.4±3.8	204.4±5.5	123.6±3.7	121.7±4.5	96.5±2.6	101.6±3.7
4	145.6±4	211.3±7.9	138.1±5.0	137.2±5.8	108.1±5.3	118.8±3.3
5	152.1±3.8	211.4±8.7	147.7±5.6	144.1±6.1	112.8±6.8	127.2±3.1
6	155.8±3.6	205.6±9.4	153.4±5.8	145.5±6.0	114.0±6.9	127.5±3.1
7	157.0±3.4	200.5±8.5	156.6±6.7	147.5±6.5	108.6±7.6	120.1±3.7
8	161.5±3.5	200.4±7.6	157.5±5.4	146.8±7.2	106.2±8.2	111.8±3.0
9	162.1±3.9	196.4±10.1	160.6±4.3	147.5±7.6	105.4±9.2	106.0±3.5
10	162.6±4.5	193.1±7.3	161.8±5.4	147.2±7.6	105.1±9.3	101.0±3.8
11	168.3±3.8	199.3±7.1	168.2±5.8	148.8±8.0	106.1±10.4	97.5±3.6
12	172.8±4.3	195.2±6.4	172.2±6.6	150.1±8.7	108.7±10.2	94.7±5.1
13	175.3±4.9	193.6±7.6	171.0±6.4	151.6±9.0	112.2±9.9	101.1±6.8
14	177.4±4.7	193.4±5.9	171.0±6.2	150.3±8.9	112.2±9.6	99.4±6.8
15	178.5±5.3	197.4±6.5	171.6±4.6	150.2±10.0	115.2±9.0	100.6±7.9
16	179.3±4.9	194.8±4.7	171.9±5.1	152.5±10.4	116.6±8.8	104.2±9.8
17	179.1±4.7	185.0±5.8	172.2±4.8	151.3±10.0	119.8±9.7	105.8±10.7
18	179.7±4.5	183.9±4.6	172.8±4.1	151.3±9.6	120.2±9.7	105.0±11.1
19	175.7±6.0	182.2±5.5	169.4±3.4	150.3±9.1	117.3±9.4	105.2±11.3
20	177.8±5.7	180.8±5.0	168.3±4.6	149.7±9.2	121.0±9.3	102.9±10.6
21	176.1±5.5	182.1±5.3	168.9±5.1	149.1±10.4	117.3±9.5	102.3±11.4
22	174.5±5.4	179.7±5.2	171.0±6.8	144.4±9.4	116.3±8.9	102.6±11.4
23	174.7±5.6	182.4±4.7	171.7±7.5	142.6±8.0	118.2±8.2	104.2±12.8
24	177.2±5.2	178.2±6.5	171.3±7.1	142.6±7.7	117.1±8.2	99.7±11.7
25	173.7±6.1	172.3±7.4	173.3±7.7	140.1±7.9	114.1±6.8	95.4±11.4
26	171.3±6.3	174.4±7.6	170.4±6.3	139.3±8.2	112.3±6.3	96.8±12.7

27	166.2±6.2	173.0±7.6	166.3±6.1	135.1±7.5	111.0±7.2	86.9±10.7
28	168.1±7.0	169.3±8.5	164.9±6.7	133.6±6.7	112.8±7.4	86.9±11.1
29	168.1±6.1	170.5±9.1	167.6±7.0	131.2±7.2	111.8±7.7	85.4±11.5
30	166.6±6.2	166.9±8.8	166.4±6.9	128.3±6.8	110.5±7.8	82.1±11.3
31	164.3±6.5	165.6±7.8	164.5±5.9	126.6±7.5	110.4±7.9	81.1±11.6
32	162.7±6.4	160.2±7.7	161.7±4.7	125.7±7.4	105.7±6.4	76.8±11.2
33	163.2±6.5	160.1±7.9	162.9±4.9	120.6±7.6	103.7±6.3	74.1±10.5
34	158.1±6.1	156.3±6.8	162.4±4.7	119.1±7.1	102.3±5.5	74.2±10.7
35	155.0±6.7	149.8±5.6	159.9±4.2	118.6±6.7	100.0±5.6	70.8±9.9
36	154.7±6.1	203.6±6.2	156.6±5.1	118.8±7.2	101.3±5.6	70.2±9.8
37	152.9±5.6	205.4±6.6	152.9±5.0	118.7±7.0	98.8±4.9	69.5±9.5
38	150.9±5.2	204.4±4.0	151.5±5.3	118.7±6.4	98.9±3.7	69.3±9.3
39	149.5±5.4	211.3±4.1	149.7±5.6	116.9±6.1	95.1±3.1	68.9±9.0
40	149.2±5.4	211.4±2.7	149.7±6.3	114.1±5.7	92.5±2.8	68.5±8.5
41	152.3±6.6	205.6±2.9	150.8±6.4	113.4±5.4	91.5±3.0	65.3±7.8
42	152.1±6.4	200.5±5.1	147.5±6.4	111.4±4.7	88.7±3.7	66.9±8.3
43	151.3±5.8	200.4±6.4	149.0±6.2	110.9±4.8	89.7±3.5	65.7±7.7
44	153.1±6.2	196.4±5.2	149.3±7.5	109.6±4.8	86.2±3.2	66.2±7.8
45	150.8±5.5	193.1±5.0	147.3±7.9	108.1±5.0	85.9±3.2	66.5±7.7
46	151.5±6.4	199.3±3.7	146.1±7.9	108.0±5.3	79.7±2.9	66.4±7.6
47	145.9±5.9	195.2±6.0	144.2±8.1	109.0±5.7	79.9±3.0	64.7±6.8
48	146.7±6.6	193.6±7.1	144.0±9.2	107.9±6.0	78.3±4.3	63.8±6.8

3.2. Sandwiching method on DMA

This chapter and related sections are under review in Advanced Functional Materials.

3.2.1 Concept of sandwiching method

The sandwiching technique for open format droplet arrays allows parallel manipulation of liquid within nanodroplets on the DMA platform. Here is a simplified overview of the process (Figure 19). Using a DMA surface as a receiver slide, 672 droplets are precisely deposited. A donor slide of the same size as the DMA is positioned over the receiver slide, allowing selective removal of volume based on its hydrophilic pattern. The process takes approximately 10 seconds, which can be used for cell media uptake, spherical cell transfer, and LDH enzyme assay sample analysis.

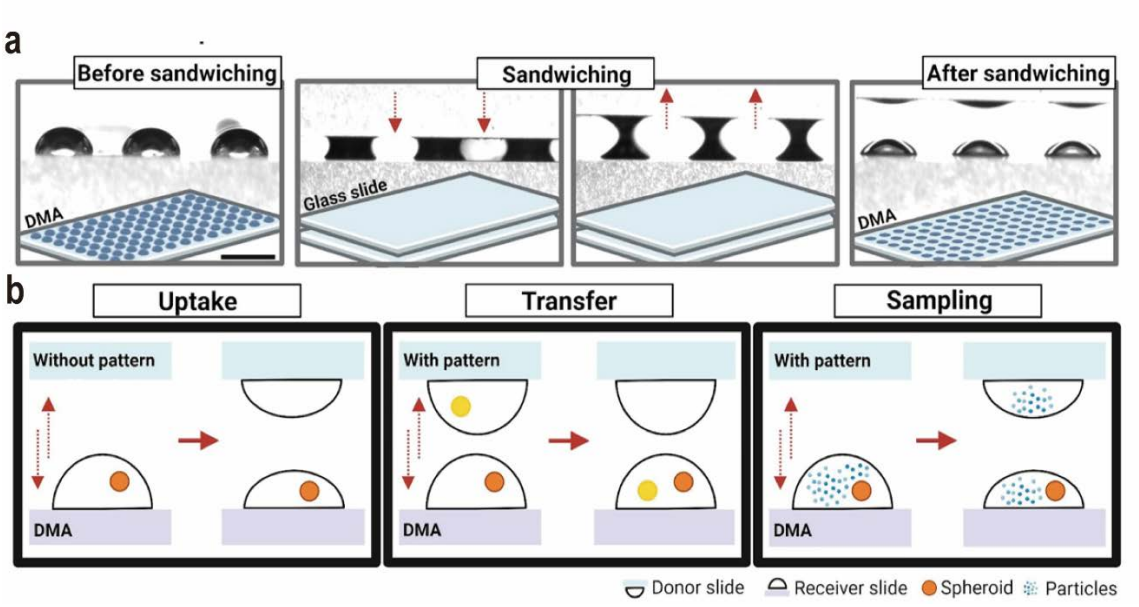

Figure 19. Concept of sandwiching method. a) A workflow of sandwiching method. A sandwich structure was created by placing a slider on top of the DMA. Then the liquid can move from bottom to top. b) Application of sandwiching method.

3.2.2 Long-term cell culture of adherence cells

To facilitate the sandwiching technique, a custom adapter with adjustable heights was designed by Joaquin E. Urrutia Gomez. The DMA slide was positioned at the bottom of the adapter with the droplet facing inward, while the HEMA-EDMA slide was carefully placed over the adapter with its coated surface facing downward toward the DMA. The use of 0.4 mm spacers prevented direct contact between the sliding surfaces, thereby preventing adjacent droplets from inadvertently merging. Joaquin E. Urrutia Gomez has confirmed that the use of this adapter can result in the removal of nearly 50% of the liquid from the DMA using the HEMA-EDMA slide.

I used this adapter to validate the feasibility of the sandwiching experimental method for long-term cell culture. HeLa CCL2 cells were initially selected for a long-term culture study. The DMA was disinfected with 100% alcohol and air dried under a clean bench for at least 10 minutes. Using a non-contact dispenser, cells were seeded onto DMA at 10 and 100 cells in 300 nL droplets, then placed in a pre-prepared Petri dish with PBS to prevent evaporation and incubated for 24 hours. After 24 hours, the first medium change was performed. The HEMA-EDMA slide was also disinfected with 100% alcohol and air dried before being used in the sandwiching method to partially remove the medium from the DMA. After sandwiching, the DMA was quickly placed under the dispenser to add 150 nL of culture medium. The medium was changed every 24 hours for 6 days, and on day 7 the cells were stained with Hoechst, PI, and Calcein AM to observe viability.

Figure 20 shows that both low and high initial cell counts (10 and 100 cells in 300 nL, respectively) benefited from the medium exchange process in DMA platforms, showing improved cell proliferation and

survival rates. Specifically, cells that underwent sandwich medium exchange showed a significant increase in viability - 50% for the lower count and 50% for the higher count, compared to much lower rates that occurred without medium exchange. Results showed that DMAs with medium exchange had more cells and better growth compared to those without, and cell viability showed higher survival rates in DMAs where medium was exchanged, demonstrating the effectiveness of our method for long-term adherent cell culture in nanoscale droplets.

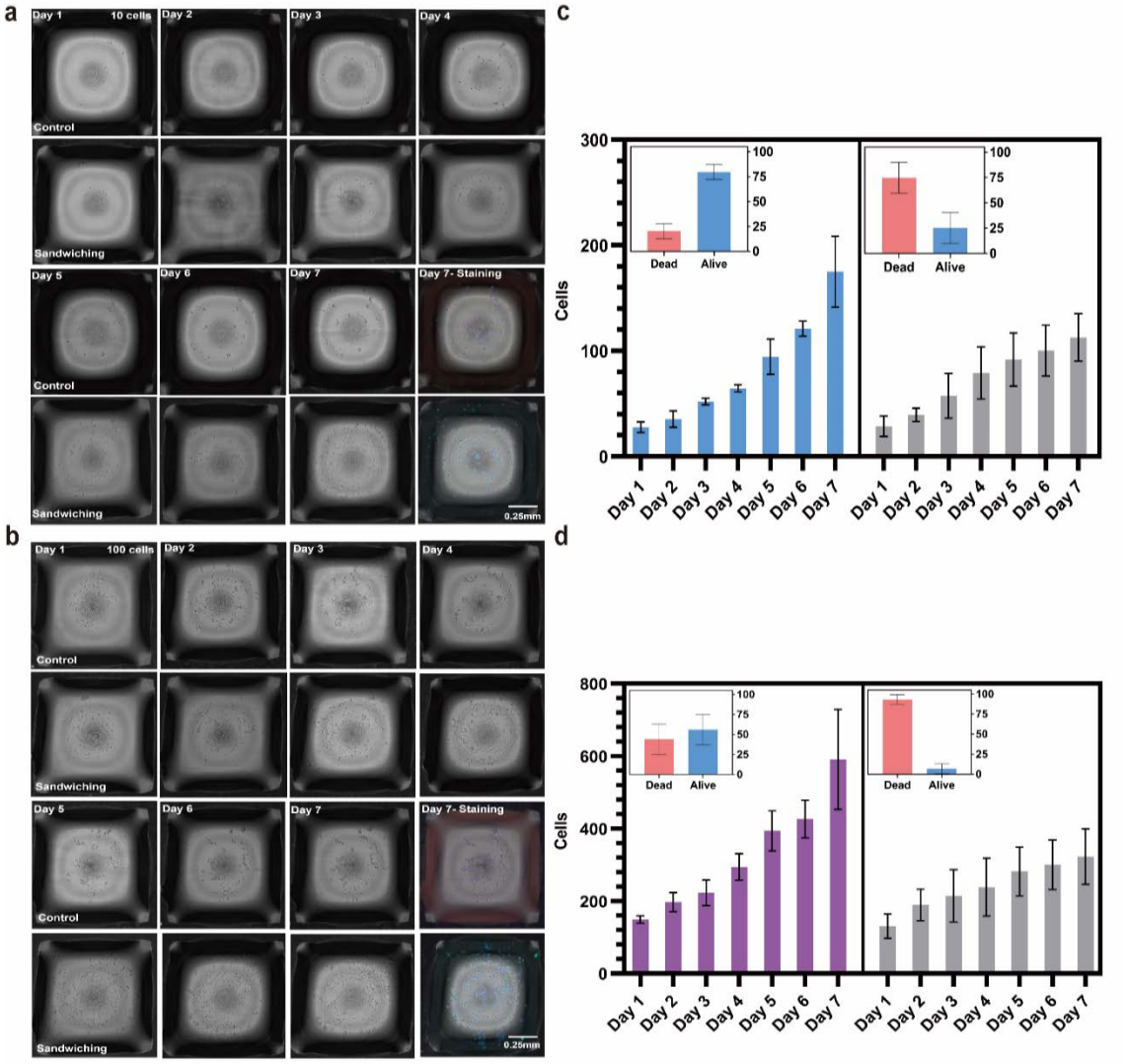

Figure 20. Long-term cell culture of adherence cells. a) Images of 7 days HeLa CCL2 cell culture by using sandwiching method (10 cells in 300 nL).

b) Images of 7 days HeLa CCL2 cell culture by using sandwiching method (100 cells in 300 nL). c) Calculating the cell number and cell viability of HeLa CCL2 cells every day (10 cells in 300 nL). d) Calculating the cell number and cell viability of HeLa CCL2 cells every day (100 cells in 300 nL). (n=3).

3.2.3 Long-term cell culture of suspension cells

To investigate the feasibility of long-term culturing suspension cells on DMA using the sandwiching method, SU-DHL4 cells were chosen. 10 and 100 cells in 300 nL were seeded by using a non-contact dispenser, then the cells underwent regular medium exchanges with a prior disinfection of the HEMA-EDMA slide. This cycle was repeated every 24 hours for 6 days. On the 7th day, cell viability was assessed.

The results, as depicted in Figure 21a - d, highlighted improved proliferation and survival rates, particularly noticeable in lower cell densities with a viability increase up to 45%. Remarkably, even at low concentrations of suspension cells without higher viability compared to the control group, there's a significant increase in cell number after 7 days of culture. This proliferation rate is up to threefold higher compared to the control group. Figure 21e shows that although there was a minimal cell loss during the sandwiching process, the method still significantly enhanced cell numbers, underscoring the technique's efficacy for long-term suspension cell culture in nanoscale droplets.

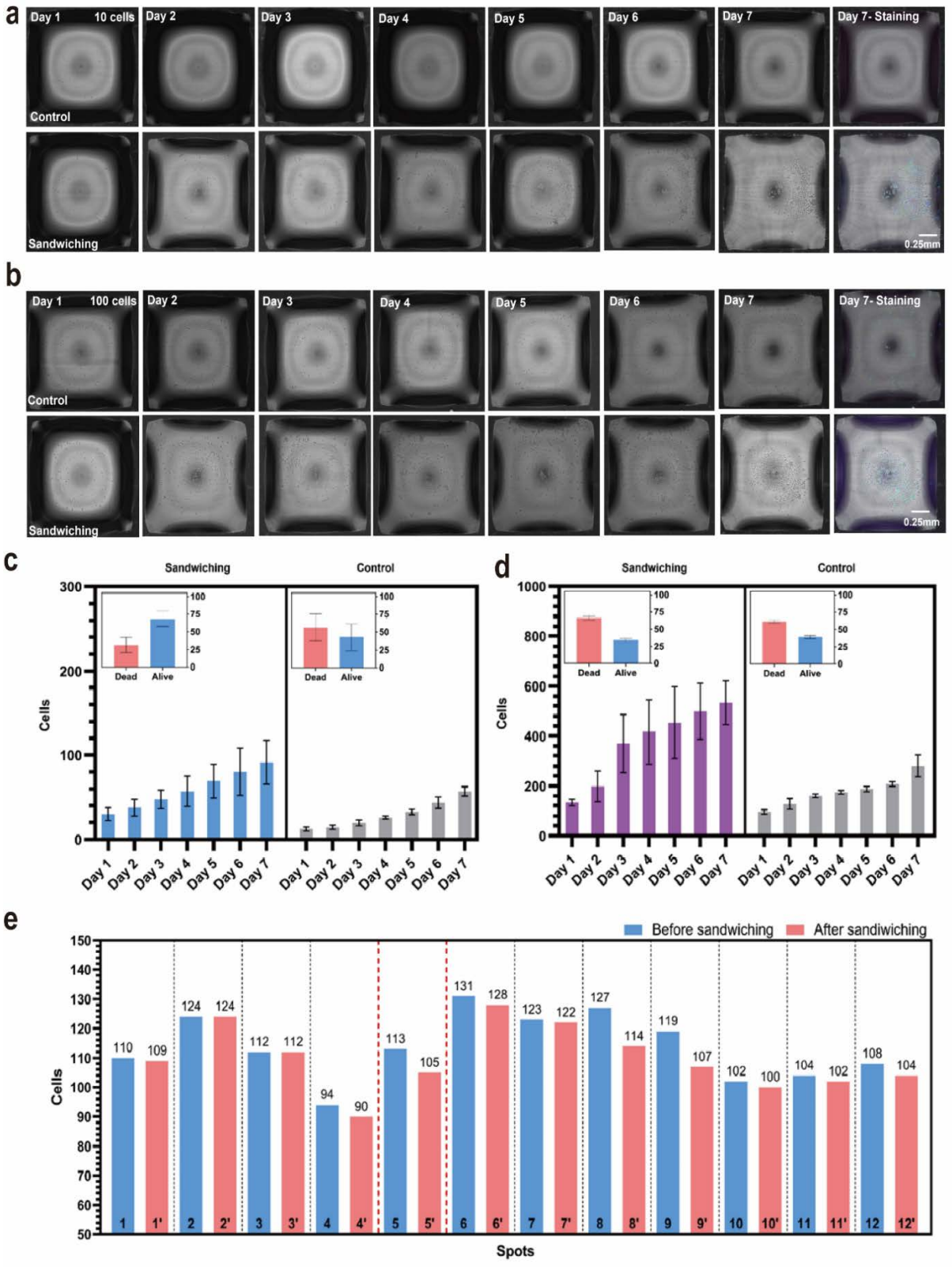

Figure 21. Long-term cell culture of suspension cells. a) Images of 7 days SU-DHL4 cell culture by using Sandwiching method (10 cells in 300

nL). b) Images of 7 days SU-DHL4 cell culture by using sandwiching method (100 cells in 300 nL). c) Calculating the cell number and cell viability of SU-DHL4 cells (10 cells in 300 nL). d) Calculating the cell number and cell viability of SU-DHL4 cells (100 cells in 300 nL). e) Calculating the cell number before and after sandwiching method. (n=3).

3.2.4 Sandwiching method for co-culture 3D cells to 2D cells

To explore additional applications of the sandwiching method, I conducted an experiment in which 3D cell culture was performed on one DMA and 2D cell culture on another DMA to investigate the feasibility of 2D-3D co-culture. After 48 hours of culture, 3D cells were transferred to the 2D cultured DMA using the sandwiching method, followed by 24 hours of co-culture to observe the interactions between the 2D and 3D cells. The workflow is shown in Figure 22a, with cell growth before the sandwiching method in Figure 22b and the co-cultured spheroid with 2D cells in Figure 22c, where staining is shown after one day of co-culture. All results indicated the possibility of 2D-3D co-culture using the sandwiching method.

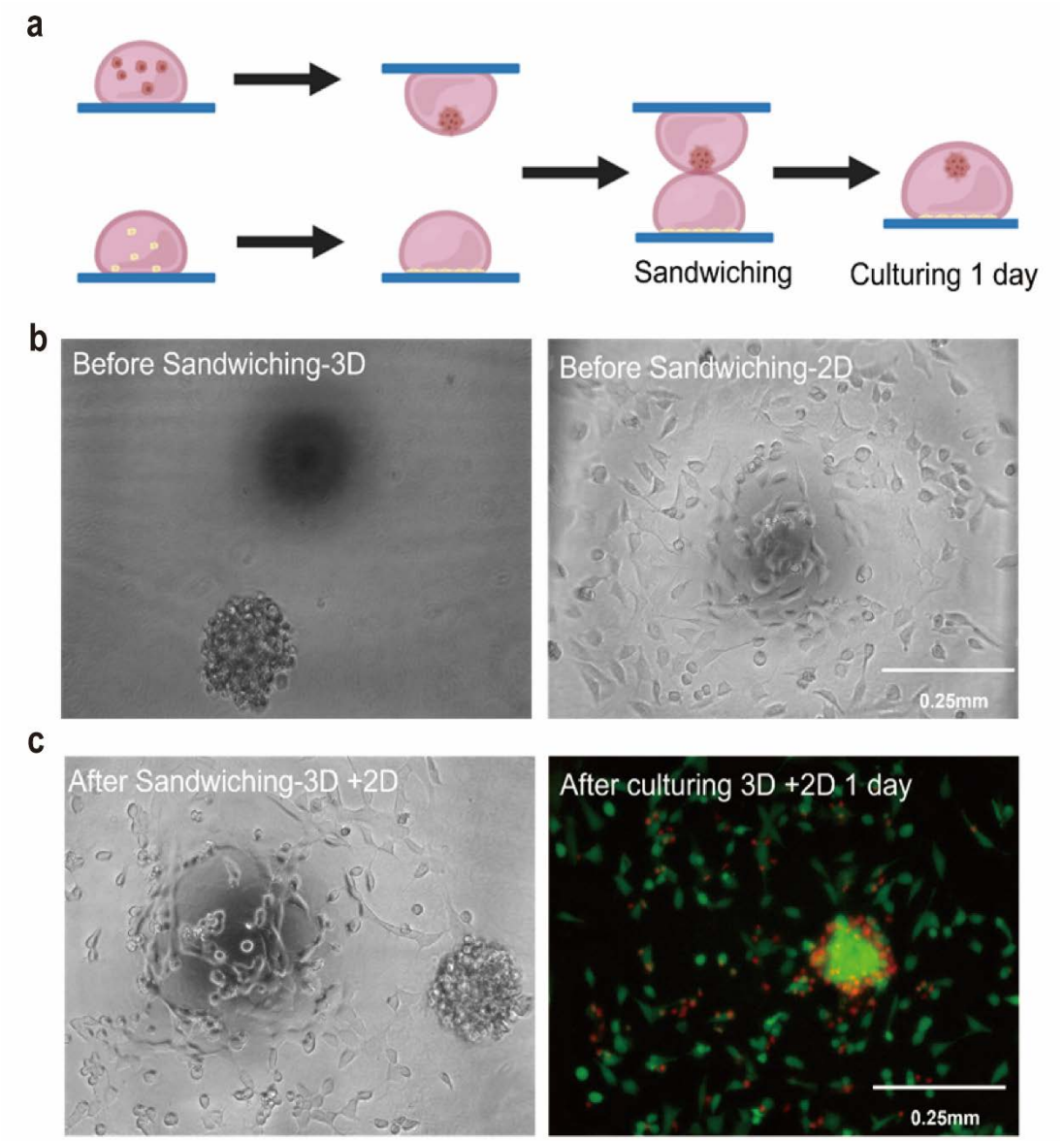

Figure 22. Sandwiching method for co-culture 3D cells to 2D cells. a) Workflow of 2D-3D cell co-culture. b) Image of before sandwiching 2D and 3D cells. c) Image of after sandwiching 2D-3D cell co-culture. Staining by Calcein AM (green), PI (red).

3.2.5 LDH test by using sandwiching method

To further explore the applications of the sandwiching method, I evaluated lactate dehydrogenase (LDH) release using this technique. By seeding 300 cells in 300 nL on a DMA and treating with 50 nL etoposide (final concentration 20 µM) for 48 hours, I then transferred the culture suspension to a fresh DMA for the LDH assay. The results in Figure 23 show higher LDH release in etoposide-treated cells compared to untreated cells, demonstrating the utility of the sandwiching method for LDH release assays.

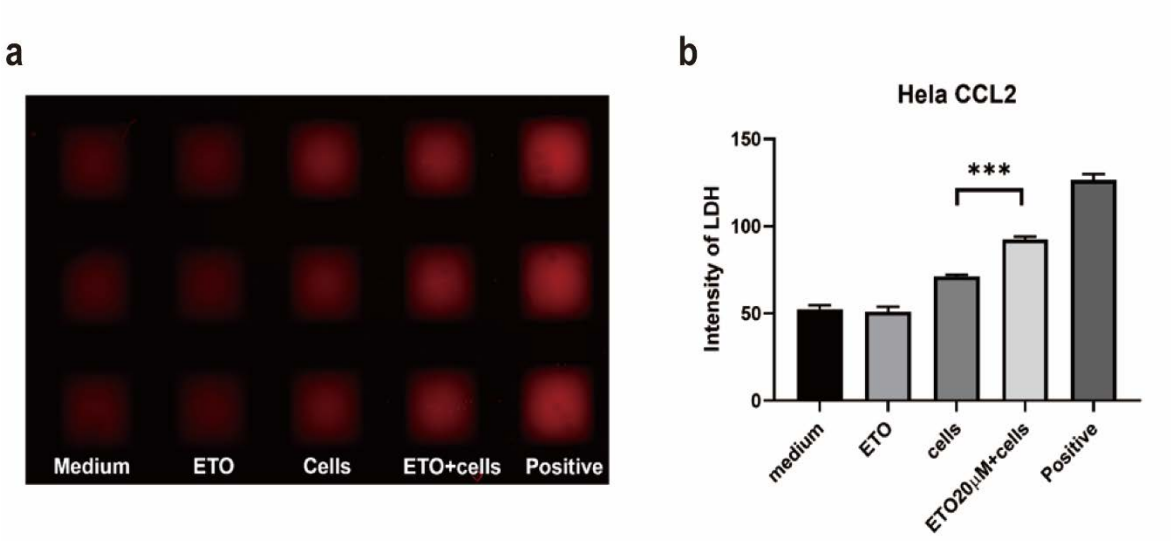

Figure 23. LDH test by using sandwiching method. a) The image of intensity of LDH. b) Calculating intensity of LDH. (mean ± sem, n=3, * P ≤ 0.05, ** P ≤ 0.01, *** P ≤ 0.001, **** P ≤ 0.0001).

3.2.6 Assessing the durability of the sandwiching method

To determine the maximum duration of cell culture using this experimental approach, I initiated a long-term culture of HeLa CCL2 cells, seeding 10 cells in 300 nL per droplet and changing the medium every two days. The cell counts consistently increased, as shown in Figure 24a and c. However, by day 14, cell viability dropped to 25%. Bright field images from Figure 24a and b suggest a significant increase in cell death between days 8 and 10, indicating that the optimal duration for this method is around 8 days.

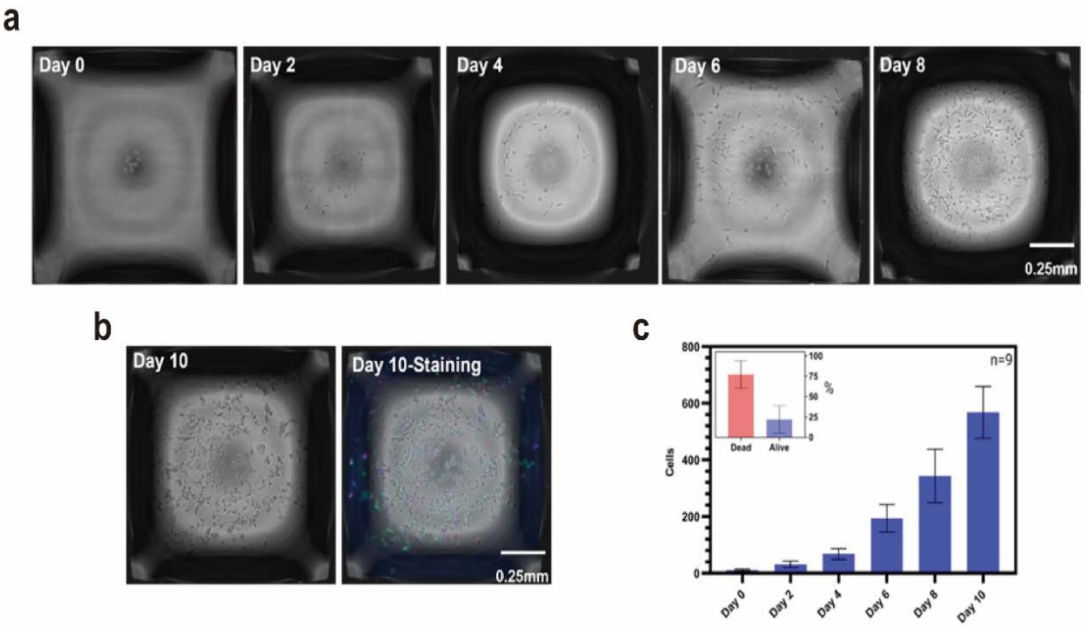

Figure 24. Assessing the durability of the sandwiching method. a) b) The image of every 2 days before medium exchange. c) Cell numbers of every 2 days. (n=3).

Chapter 4. Conclusions and outlooks

4.1 Conclusions

The dissertation shows two innovative methods for cellular analysis and culture using nanoliter droplet microarrays. The first part discusses integrating impedance spectroscopy with droplet microarrays for drug response analysis, enhancing real-time, label-free analysis (eDMA). The second part explores the use of droplet microarrays for long-term experiments, addressing the challenges of manipulating nanoliter droplets on DMA (sandwiching method). This work contributes significantly to cell biology and drug discovery, presenting new way for research and application in these fields.

In the first part, I demonstrated a miniaturized platform for real-time and label-free monitoring cell signal, which I have named eDMA. This innovative system enables parallel measurements of impedance, reflecting cell growth within 200 nL droplets through the use of impedance spectroscopy. This study presents the first demonstration of continuous impedance monitoring within nanoliter droplets for up to 48 hours. Using eDMA, I could accurately measure impedance deriving from as few as 500 cells cultured in 200 nL droplets, then successfully demonstrated parallel label-free, real-time monitoring of cellular drug response over a 48-hour period. These capabilities were validated against traditional microscopy-based assays, highlighting the ability in real-time and label-free capturing dynamic drug responses in low cell numbers within nanoliter nanoliter droplets. This technology therefore offers a significant potential for assessing the drug response of cells with limited availability, as for example physiologically relevant cells, such as patient-derived primary cells or challenging-to-culture stem cells. Our system presents itself as a

potent tool in the realms of drug discovery and personalized medicine, where real-time data and miniaturized sample requirements are crucial.

In the second part, my objective was to develop a novel method of DMA technology for manipulating nanoliter liquids. This method aims to address the specific challenges associated with conducting long-term experiments using DMA platforms. By employing a sandwiching structure combining HEMA-co-EDMA slides with DMA, I facilitate medium renewal, thereby enabling the extended cell culture times on DMA. It proves the platform's capability to support various cell types, including adherent and suspension cells for up to 7 days or more, providing a novel approach for long-term cell cultivation in nanoliter volumes. Additionally, this technique enables to transfer of cells from one slide to another for the purpose of cell co-culture, thereby studying the interaction among different cell types by nanoliter format. For further, it allows for low-interference sample analysis, such as lactate dehydrogenase (LDH) testing. This method is designed to be compatible with standard laboratory microscopy, ensuring ease of observing cell behavior by standard laboratory microscopy. This compatibility with basic assay methods emphasizes its utility in assessing cell viability and cytotoxicity. It becomes a valuable tool for high-throughput experiments and integrative biology studies.

4.2 Outlook

In the first part, the outlook of eDMA includes the reduction of droplet evaporation, increasing the capacity for analyzing a greater number of droplets, and amplifying the sensitivity of microelectrodes. These advancements are expected to enhance the utility of eDMA across various scientific fields, paving the way for high-throughput cellular studies.

First major area of development is reducing droplet evaporation leading to maintaining droplet stability for longer periods of time. This is critical because maintaining the integrity and consistency of droplets over extended periods is essential for obtaining reliable measurements and ensuring reproducibility. Reduction of droplet evaporation will prevent issues such as evaporation, coalescence, or contamination, which can compromise experimental results.

Second area of development is on increasing the throughput of eDMA for analyzing a greater number of droplets simultaneously. Currently, the eDMA system can handle around 20 droplets, but in the future, this number could expand to 100 droplets or more. This will significantly increase the system's throughput, making it more suitable for high-throughput research applications. A higher droplet capacity will allow to conduct more experiments in parallel and enables large-scale screening studies that were previously impractical.

Last area of development is improving the sensitivity of microelectrodes used within the eDMA system. Enhancing electrode sensitivity is important for detecting subtle changes in cellular behavior and interactions, thus providing more detailed and accurate data. Future improvements are expected to refine the size and sensitivity of these electrodes further, facilitating the study of both suspension cells and cell

spheroids. These improvements will be critical for gaining new insights into intercellular communication.

In the second part, the sandwiching method in the future, several key challenges can be addressed to increase the potential and practicality of DMA.

The current sandwiching method supports cell cultures on DMA for at least 7 days, but the possibility exists to extend this period, which will be contribute for studying long-term cellular behaviors and interactions. To achieve this, addressing unresolved challenges such as optimizing nutrient gradients, improving waste management. Longer culture periods will enable researchers to observe processes such as differentiation, maturation, and long-term responses to treatments.

Moreover, future improvements may involve enabling to split cells on droplets, improving methods to transfer more culture medium to keep cells viable for longer periods of time, and developing automated systems for more efficient media exchange. The development of automated systems for more efficient media exchange, reducing manual intervention and minimizing the risk of contamination. Automated media exchange systems will ensure that cells receive a constant supply of nutrients while waste products are efficiently removed, maintaining an optimal environment for cellular growth and activity. These improvements will not only address the pressing need for optimized long-term culture conditions but also unlock new possibilities for dynamic cellular studies.

In summary, these advances are expected to significantly enhance the utility of DMA in a variety of scientific studies, allowing for a deeper understanding of cellular behavior and interactions.

Curriculum Vitae

Personal data	
Name	Meijun Zhou
Email	meijun.zhou@kit.edu
Address	Hermann-von-Helmholtz-Platz 1, 76344 Eggenstein-Leopoldshafen, Germany
Education	
2020-present	PhD studies Karlsruhe Institute of Technology (KIT), Germany Institute of Biological and Chemical Systems (IBCS) Research Topic: Nanoliter Droplet Microarrays Combines with Impedance Spectroscopy and Long-Term Cell Culture for Advancement in Miniaturized Cell culture and Screening
2017-2020	Master studies Chinese Academy of Medical Sciences and Peking Union Medical College, Institute of Basic Medical Sciences, Tsinghua, Beijing, China Research Topic: Roles of Pyroptosis and BMPRII Signaling Pathway in the Pathogenesis of Systemic Lupus Erythematosus Associated Pulmonary Arterial Hypertension (SLE-PAH)

-

Publications

1. **Zhou, M**., Gomez, J. E.U., Mandsberg, N.K, Liu, S., Schmidt, S., Meier, M., Levkin, P.A., Jahnke, H.-G., and Popova, A. Electrode Droplet Microarray (eDMA): an impedance platform for label-free parallel monitoring of cellular drug response in nanoliter droplets. *Under review in Advanced Healthcare Materials.*

2. Gomez, J. E. U[§]., **Zhou, M**[§]., Serna, J.A., Liu, S., Levkin, P.A., and Popova, A. Highly Parallel Nanoliter-Scale Liquid, Cell, and Spheroid Manipulation on Droplet Microarray via Sandwiching Method. §These authors contributed equally to this work. *Under review in Advanced Functional Materials.*

3. EL Faraj, R.E.K., Chakraborty, S., **Zhou, M**., Sobol, M., Thiele, D., ShatfordAdams, L., Cassal, M., Kaster, A., Dietrich, S., Levkin, P.A., and Popova, A. Drug-Induced Differential Gene Expression Analysis on Nanoliter Droplet Microarrays: Enabling Tool for Functional Precision Oncology. *Under review in Advanced Healthcare Materials.*

4. Zhang, J., Liu, S., Kanokkanchana, K., Kuzina, M., **Zhou, M**., Du, X., Plumere, N., Gu, Z., Dong, Z., Levkin, P.A. Fabrication of 3D Functional Nanocomposites through Post-Doping of Two-Photon Microprinted Nanoporous Architectures. *Under review in Small.*

References

1 Hudu, S. A., Alshrari, A. S., Syahida, A. & Sekawi, Z. Cell Culture, Technology: Enhancing the Culture of Diagnosing Human Diseases. *Journal of Clinical and Diagnostic Research* 10, DE01-05(2016).

2 Willmer, E. N. *Cells and tissues in culture: methods, biology and physiology*. (Elsevier, 2015).

3 Adams, R. L. P. *Cell culture for biochemists*. (Elsevier, 1990).

4 Butler, M. *Animal cell culture and technology*. (Taylor & Francis, 2004).

5 Thorpe, T. A. History of plant tissue culture. *Mol Biotechnol* 37, 169-180 (2007).

6 Jedrzejczak-Silicka, M. History of cell culture. *New insights into cell culture technology* 1, 13 (2017).

7 Freshney, R., Obradovic, B., Grayson, W. & Cannizzaro, C. Principles of tissue culture and bioreactor design. *Principles of tissue engineering*, 155-183 (2007).

8 Anaya, J.-M., Shoenfeld, Y., Rojas-Villarraga, A., Levy, R. A. & Cervera, R. Autoimmunity: from bench to bedside. (2013).

9 McKinnon, K. M. Flow cytometry: an overview. *Current protocols in immunology* 120, 5.1. 1-5.1. 11 (2018).

10 Adan, A., Alizada, G., Kiraz, Y., Baran, Y. & Nalbant, A. Flow cytometry: basic principles and applications. *Critical reviews in biotechnology* 37, 163-176 (2017).

11 Rieseberg, M., Kasper, C., Reardon, K. F. & Scheper, T. Flow cytometry in biotechnology. *Applied microbiology and biotechnology* 56, 350-360 (2001).

12 Morris, J. D. & Payne, C. K. Microscopy and cell biology: new methods and new questions. *Annual review of physical chemistry* 70, 199-218 (2019).

13 Patel, D. V. & McGhee, C. N. Quantitative analysis of in vivo confocal microscopy images: a review. *Survey of ophthalmology* 58, 466-475 (2013).

14 Verschueren, H. Interference reflection microscopy in cell biology: methodology and applications. *Journal of cell science* 75, 279-301 (1985).

15 Wulfkuhle, J., Espina, V., Liotta, L. & Petricoin, E. Genomic and proteomic technologies for individualisation and improvement of cancer treatment. *European Journal of Cancer* 40, 2623-2632 (2004).

16 Tainsky, M. A. Genomic and proteomic biomarkers for cancer: a multitude of opportunities. *Biochimica et Biophysica Acta (BBA)-Reviews on Cancer* 1796, 176-193 (2009).

17 Mahboubi, A. A., Akhoundi, M. M. & Sadeghi, M. R. Application of genomic and proteomic technologies to early detection of cancer. *Archives of Iranian Medicine* 11, 427-434 (2008).

18 Diederichsen, A. C. *et al.* Flow cytometric investigation of immune-response-related surface molecules on human colorectal cancers. *International journal of cancer* 79, 283-287 (1998).

19 Cattin, S. *et al.* Circulating immune cell populations related to primary breast cancer, surgical removal, and radiotherapy revealed by flow cytometry analysis. *Breast Cancer Research* 23, 64 (2021).

20 Verronèse, E. *et al.* Immune cell dysfunctions in breast cancer patients detected through whole blood multi-parametric flow cytometry assay. *Oncoimmunology* 5, e1100791 (2016).

21 Barlogie, B. *et al.* Flow cytometry in clinical cancer research. *Cancer research* 43, 3982-3997 (1983).

22 Georgakoudi, I. *et al.* In vivo flow cytometry: a new method for enumerating circulating cancer cells. *Cancer research* 64, 5044-5047 (2004).
23 Liu, A. Y. *et al.* Analysis and sorting of prostate cancer cell types by flow cytometry. *The Prostate* 40, 192-199 (1999).
24 Bajgelman, M. C. in *Data processing handbook for complex biological data sources* 119-124 (Elsevier, 2019).
25 Maciorowski, Z., Chattopadhyay, P. K. & Jain, P. Basic multicolor flow cytometry. *Current protocols in immunology* 117, 5.4. 1-5.4. 38 (2017).
26 Telford, W. G., Hawley, T., Subach, F., Verkhusha, V. & Hawley, R. G. Flow cytometry of fluorescent proteins. *Methods* 57, 318-330 (2012).
27 Baird, W. V., Estager, A. S. & Wells, J. K. Estimating nuclear DNA content in peach and related diploid species using laser flow cytometry and DNA hybridization. *Journal of the American Society for Horticultural Science* 119, 1312-1316 (1994).
28 Lian, H., He, S., Chen, C. & Yan, X. Flow cytometric analysis of nanoscale biological particles and organelles. *Annual Review of Analytical Chemistry* 12, 389-409 (2019).
29 Young, M. R. Principles and Technique of Fluorescence Microscopy. *Journal of Cell Science* s3-102, 419-449(1961).
30 Rane, A. S., Rutkauskaite, J., deMello, A. & Stavrakis, S. High-throughput multi-parametric imaging flow cytometry. *Chem* 3, 588-602 (2017).
31 Walker, L. A. *et al.* CLEAR: coverage-based limiting-cell experiment analysis for RNA-seq. *Journal of Translational Medicine* 18, 63 (2020).
32 Erickson-Miller, C. L. *et al.* Discovery and characterization of a selective, nonpeptidyl thrombopoietin receptor agonist. *Experimental Hematology* 33, 85-93 (2005).
33 Lemm, J. A. *et al.* Identification of Hepatitis C Virus NS5A Inhibitors. *Journal of Virology* 84, 482-491 (2010).
34 Gao, Z. *et al.* An RNA polymerase II- and AGO4-associated protein acts in RNA-directed DNA methylation. *Nature* 465, 106-109 (2010).
35 Keserü, G. M. & Makara, G. M. The influence of lead discovery strategies on the properties of drug candidates. *Nature Reviews Drug Discovery* 8, 203-212 (2009).
36 Popova, A. A. *et al.* Miniaturized Drug Sensitivity and Resistance Test on Patient-Derived Cells Using Droplet-Microarray. *SLAS TECHNOLOGY: Translating Life Sciences Innovation* 26, 274-286 (2021).
37 Seifermann, M., Reiser, P., Friederich, P. & Levkin, P. A. High-Throughput Synthesis and Machine Learning Assisted Design of Photodegradable Hydrogels. *Small Methods* 7, 2300553 (2023).
38 Lu, Y. *et al.* Emerging Pharmacotherapeutic Strategies to Overcome Undruggable Proteins in Cancer. *International journal of biological sciences* 19, 3360-3382 (2023).
39 Panwar, J., Utharala, R., Fennelly, L., Frenzel, D. & Merten, C. A. iSort enables automated complex microfluidic droplet sorting in an effort to democratize technology. *Cell Reports Methods* 3, 100478 (2023).
40 Astashkina, A., Mann, B. & Grainger, D. W. A critical evaluation of in vitro cell culture models for high-throughput drug screening and toxicity. *Pharmacology & therapeutics* 134, 82-106 (2012).
41 Malo, N., Hanley, J. A., Cerquozzi, S., Pelletier, J. & Nadon, R. Statistical

practice in high-throughput screening data analysis. *Nature Biotechnology* 24, 167-175 (2006).
42 Goktug, A. N., Chai, S. C. & Chen, T. Data analysis approaches in high throughput screening. *Drug Discovery*, 201-226 (2013).
43 Popova, A. A. *et al.* Facile One Step Formation and Screening of Tumor Spheroids Using Droplet-Microarray Platform. *Small* 15, 1901299 (2019).
44 Feng, W. *et al.* Surface Patterning via Thiol-Yne Click Chemistry: An Extremely Fast and Versatile Approach to Superhydrophilic-Superhydrophobic Micropatterns. *Advanced Materials Interfaces* 1, 1400269 (2014).
45 Brehm, M., Heissler, S., Afonin, S. & Levkin, P. A. Nanomolar Synthesis in Droplet Microarrays with UV-Triggered On-Chip Cell Screening. *Small* 16, 1905971 (2020).
46 Chakraborty, S. *et al.* "Cells-to-cDNA on Chip": Phenotypic Assessment and Gene Expression Analysis from Live Cells in Nanoliter Volumes Using Droplet Microarrays. *Advanced Healthcare Materials* 11, 2102493 (2022).
47 Cui, H. *et al.* High-throughput formation of miniaturized cocultures of 2D cell monolayers and 3D cell spheroids using droplet microarray. *Droplet* 2, e39 (2023).
48 Lei, W., Demir, K., Overhage, J., Grunze, M., Schwartz, T., Levkin, PA. Droplet-Microarray: Miniaturized Platform for High-Throughput Screening of Antimicrobial Compounds. *Advanced Biosystems* 4 (2020).
49 Liu, Y. *et al.* Droplet microarray based screening identifies proteins for maintaining pluripotency of hiPSCs. *Advanced Healthcare Materials* 11, 2200718 (2022).
50 Tronser, T., Demir, K., Reischl, M., Bastmeyer, M. & Levkin, P. A. Droplet microarray: miniaturized platform for rapid formation and high-throughput screening of embryoid bodies. *Lab Chip* 18, 2257-2269 (2018).
51 Tronser, T., Popova, A. A., Jaggy, M., Bastmeyer, M. & Levkin, P. A. Droplet microarray based on patterned superhydrophobic surfaces prevents stem cell differentiation and enables high-throughput stem cell screening. *Advanced Healthcare Materials* 6, 1700622 (2017).
52 Tronser, T., Popova, A. A. & Levkin, P. A. Miniaturized platform for high-throughput screening of stem cells. *Current opinion in biotechnology* 46, 141-149 (2017).
53 Liu, Y. *et al.* Miniaturized droplet microarray platform enables maintenance of human induced pluripotent stem cell pluripotency. *Materials Today Bio* 12, 100153 (2021).
54 Popova, A. A. *et al.* Miniaturized Drug Sensitivity and Resistance Test on Patient-Derived Cells Using Droplet-Microarray. *SLAS Technology* 26, 274-286 (2021).
55 Cui, H. *et al.* Repurposing FDA-approved drugs for temozolomide-resistant IDH1 mutant glioma using high-throughput miniaturized screening on droplet microarray chip. *Advanced Healthcare Materials* 12, 2300591 (2023).
56 Popova, A. A. & Levkin, P. A. Precision medicine in oncology: in vitro drug sensitivity and resistance test (DSRT) for selection of personalized anticancer therapy. *Advanced Therapeutics* 3, 1900100 (2020).
57 Tian, Y. *et al.* High-Throughput Miniaturized Synthesis of PROTAC-Like Molecules. *Small* , 2307215 (2024).

58 Gao, X. & Jiang, L. Water-repellent legs of water striders. *Nature* 432, 36-36 (2004).
59 Law, K.-Y. Definitions for Hydrophilicity, Hydrophobicity, and Superhydrophobicity: Getting the Basics Right. *The Journal of Physical Chemistry Letters* 5, 686-688 (2014).
60 Geyer, F. L., Ueda, E., Liebel, U., Grau, N. & Levkin, P. A. Superhydrophobic-superhydrophilic micropatterning: towards genome-on-a-chip cell microarrays. *Angewandte Chemie International Edition* 50, 8424-8427 (2011).
61 Oudeng, G. *et al.* Droplet Microarray Based on Nanosensing Probe Patterns for Simultaneous Detection of Multiple HIV Retroviral Nucleic Acids. *ACS Applied Materials & Interfaces* 12, 55614-55623 (2020).
62 Höpfner, J., Brehm, M. & Levkin, P. A. Palladium-Catalyzed Combinatorial Synthesis of Biphenyls on Droplet Microarrays at Nanoliter Scale. *Small* 20, 2304325 (2024).
63 Wiedmann, J. J. *et al.* Nanoliter Scale Parallel Liquid–Liquid Extraction for High-Throughput Purification on a Droplet Microarray. *Small* 19, 2204512 (2023).
64 Popova, A. A. *et al.* Droplet-Array (DA) sandwich chip: a versatile platform for High-Throughput cell screening based on Superhydrophobic–Superhydrophilic micropatterning. *Advanced Materials* 27, 5217-5222 (2015).
65 Feng, W., Ueda, E. & Levkin, P. A. Droplet microarrays: from surface patterning to high-throughput applications. *Advanced Materials* 30, 1706111 (2018).
66 Sarró, E. *et al.* Real-time and on-line monitoring of morphological cell parameters using electrical impedance spectroscopy measurements. *Journal of Chemical Technology & Biotechnology* 91, 1755-1762 (2016).
67 Yang, L. *et al.* High-Throughput Methods in the Discovery and Study of Biomaterials and Materiobiology. *Chemical Reviews* 121, 4561-4677 (2021).
68 Magar, H. S., Hassan, R. Y. & Mulchandani, A. Electrochemical impedance spectroscopy (EIS): Principles, construction, and biosensing applications. *Sensors* 21, 6578 (2021).
69 Rapier, C. E., Jagadeesan, S., Vatine, G. & Ben-Yoav, H. Microfluidic channel sensory system for electro-addressing cell location, determining confluency, and quantifying a general number of cells. *Scientific Reports* 12, 3248 (2022).
70 Kadan-Jamal, K. *et al.* Electrical Impedance Spectroscopy of plant cells in aqueous biological buffer solutions and their modelling using a unified electrical equivalent circuit over a wide frequency range: 4Hz to 20 GHz. *Biosensors and Bioelectronics* 168, 112485 (2020).
71 Moghtaderi, H. *et al.* Electric cell-substrate impedance sensing in cancer research: An in-depth exploration of impedance sensing for profiling cancer cell behavior. *Sensors and Actuators Reports* 7, 100188 (2024).
72 Primiceri, E. *et al.* Real-time monitoring of copper ions-induced cytotoxicity by EIS cell chips. *Biosensors and Bioelectronics* 25, 2711-2716 (2010).
73 Caviglia, C. *et al.* Interdependence of initial cell density, drug concentration and exposure time revealed by real-time impedance spectroscopic cytotoxicity assay. *Analyst* 140, 3623-3629 (2015).
74 Crowell, L. L., Yakisich, J. S., Aufderheide, B. & Adams, T. N. Electrical impedance spectroscopy for monitoring chemoresistance of cancer cells. *Micromachines* 11, 832 (2020).
75 Amini, M., Hisdal, J. & Kalvøy, H. Applications of bioimpedance measurement

techniques in tissue engineering. *Journal of Electrical Bioimpedance* 9, 142-158 (2018).
76 Dahmen, E. A. M. F. *Electroanalysis: theory and applications in aqueous and non-aqueous media and in automated chemical control*. (Elsevier, 1986).
77 Jahnke, H.-G. *et al.* FEM-based design of optical transparent indium tin oxide multielectrode arrays for multiparametric, high sensitive cell based assays. *Biosensors and Bioelectronics* 129, 208-215 (2019).
78 Schwarz, M., Jendrusch, M. & Constantinou, I. Spatially resolved electrical impedance methods for cell and particle characterization. *Electrophoresis* 41, 65-80 (2020).
79 Arman, S., Tilley, R. D. & Gooding, J. J. A review of electrochemical impedance as a tool for examining cell biology and subcellular mechanisms: merits, limits, and future prospects. *Analyst* (2024).
80 Reppel, M. *et al.* Microelectrode arrays: A new tool to measure embryonic heart activity. *Journal of Electrocardiology* 37, 104-109 (2004).
81 Frega, M., Tedesco, M., Massobrio, P., Pesce, M. & Martinoia, S. Network dynamics of 3D engineered neuronal cultures: a new experimental model for in-vitro electrophysiology. *Scientific Reports* 4, 5489 (2014).
82 Natarajan, A., Molnar, P., Sieverdes, K., Jamshidi, A. & Hickman, J. Microelectrode array recordings of cardiac action potentials as a high throughput method to evaluate pesticide toxicity. *Toxicology in Vitro* 20, 375-381 (2006).
83 Kussauer, S., David, R. & Lemcke, H. Microelectrode Arrays: A Valuable Tool to Analyze Stem Cell-Derived Cardiomyocytes. *Stem Cells: Latest Advances*, 1-20 (2021).
84 Novak, J. L. & Wheeler, B. C. Recording from the Aplysia abdominal ganglion with a planar microelectrode array. *IEEE transactions on biomedical engineering*, 196-202 (1986).
85 Stett, A. *et al.* Biological application of microelectrode arrays in drug discovery and basic research. *Analytical and bioanalytical chemistry* 377, 486-495 (2003).
86 Tanwar, A., Gandhi, H. A., Kushwaha, D. & Bhattacharya, J. A review on microelectrode array fabrication techniques and their applications. *Materials Today Chemistry* 26, 101153 (2022).
87 Kussauer, S., David, R. & Lemcke, H. hiPSCs derived cardiac cells for drug and toxicity screening and disease modeling: what micro-electrode-array analyses can tell us. *Cells* 8, 1331 (2019).
88 Ryynänen, T. *et al.* Microelectrode array for noninvasive analysis of cardiomyocytes at the single-cell level. *Japanese Journal of Applied Physics* 57, 117001 (2018).
89 Susloparova, A. *et al.* Low impedance and highly transparent microelectrode arrays (MEA) for in vitro neuron electrical activity probing. *Sensors and Actuators B: Chemical* 327, 128895 (2021).
90 Benavente, J. Electrochemical Impedance Spectroscopy as a Tool for Electrical and Structural Characterizations of Membranes in Contact with Electrolyte Solutions. *Recent Advances in Multidisciplinary Applied Physics*, 463-471 (2005).
91 Yamamoto, W. *et al.* Electrophysiological characteristics of human iPSC-derived cardiomyocytes for the assessment of drug-induced proarrhythmic potential. *PloS one* 11, e0167348 (2016).

92 Sala, L., Ward-van Oostwaard, D., Tertoolen, L. G., Mummery, C. L. & Bellin, M. Electrophysiological analysis of human pluripotent stem cell-derived cardiomyocytes (hPSC-CMs) using multi-electrode arrays (MEAs). *Journal of Visualized Experiments*, e55587 (2017).
93 Asakura, K. *et al.* Improvement of acquisition and analysis methods in multi-electrode array experiments with iPS cell-derived cardiomyocytes. *Journal of pharmacological and toxicological methods* 75, 17-26 (2015).
94 Sharf, T. *et al.* Functional neuronal circuitry and oscillatory dynamics in human brain organoids. *Nature Communications* 13, 4403 (2022).
95 Mossink, B. *et al.* Human neuronal networks on micro-electrode arrays are a highly robust tool to study disease-specific genotype-phenotype correlations in vitro. *Stem Cell Reports* 16, 2182-2196 (2021).
96 Liu, Y. *et al.* Nanomaterial-based microelectrode arrays for in vitro bidirectional brain-computer interfaces: a review. *Microsystems & Nanoengineering* 9, 13 (2023).
97 Tasnim, K. & Liu, J. Emerging Bioelectronics for Brain Organoid Electrophysiology. *Journal of Molecular Biology* 434, 167165 (2022).
98 Striebel, J. *et al.* Human neural network activity reacts to gravity changes in vitro. *Front Neurosci* 17, 1085282 (2023).
99 Pelkonen, A. *et al.* Functional Characterization of Human Pluripotent Stem Cell-Derived Models of the Brain with Microelectrode Arrays. *Cells* 11 (2021).
100 Xiang, Z., Liu, J. & Lee, C. A flexible three-dimensional electrode mesh: An enabling technology for wireless brain–computer interface prostheses. *Microsystems & Nanoengineering* 2, 16012 (2016).
101 Faul, E.-B. A. *et al.* Batch Fabrication of Microelectrode Arrays with Glassy Carbon Microelectrodes and Interconnections for Neurochemical Sensing: Promises and Challenges. *Micromachines* 15, 277 (2024).
102 Winau, F., Westphal, O. & Winau, R. Paul Ehrlich--in search of the magic bullet. *Microbes and Infection* 6, 786-789 (2004).
103 Schwartz, R. S. Paul Ehrlich's magic bullets. *The New England Journal of Medicine* 350, 1079-1080 (2004).
104 Krantz, J. C. Historical medical classics involving new drugs (Williams & Wilkins, 1974).
105 Miller, D. R. A tribute to Sidney Farber–the father of modern chemotherapy. *British Journal of Haematology* 134, 20-26 (2006).
106 Meddings, J. B., Scott, R. B. & Fick, G. H. Analysis and comparison of sigmoidal curves: application to dose-response data. *American Journal of Physiology-Gastrointestinal and Liver Physiology* 257, G982-G989 (1989).
107 El-Kareh, A. W. & Secomb, T. W. Two-Mechanism Peak Concentration Model for Cellular Pharmacodynamics of Doxorubicin. *Neoplasia* 7, 705-713 (2005).
108 Dagogo-Jack, I. & Shaw, A. T. Tumour heterogeneity and resistance to cancer therapies. *Nature Reviews Clinical Oncology* 15, 81-94 (2018).
109 Vasan, N., Baselga, J. & Hyman, D. M. A view on drug resistance in cancer. *Nature* 575, 299-309 (2019).
110 Kumar, P., Nagarajan, A. & Uchil, P. D. Analysis of cell viability by the MTT assay. *Cold Spring Harbor Protocols* 2018, pdb. prot095505 (2018).
111 Supino, R. MTT assays. *In vitro Toxicity Testing Protocols*, 137-149 (1995).
112 Van Meerloo, J., Kaspers, G. J. & Cloos, J. Cell sensitivity assays: the MTT assay. *Cancer Cell Culture: Methods and Protocols*, 237-245 (2011).

113 Stockert, J. C., Blázquez-Castro, A., Cañete, M., Horobin, R. W. & Villanueva, Á. MTT assay for cell viability: Intracellular localization of the formazan product is in lipid droplets. *Acta Histochemica* 114, 785-796 (2012).
114 Tian, M., Ma, Y. & Lin, W. Fluorescent probes for the visualization of cell viability. *Accounts of Chemical Research* 52, 2147-2157 (2019).
115 Foglieni, C., Meoni, C. & Davalli, A. M. Fluorescent dyes for cell viability: an application on prefixed conditions. *Histochemistry and Cell Biology* 115, 223-229 (2001).
116 Chan, L. L., Wilkinson, A. R., Paradis, B. D. & Lai, N. Rapid image-based cytometry for comparison of fluorescent viability staining methods. *Journal of Fluorescence* 22, 1301-1311 (2012).
117 Pollack, A. & Ciancio, G. in *Methods in Cell Biology* Vol. 33 19-24 (Elsevier, 1990).
118 Vermes, I., Haanen, C. & Reutelingsperger, C. Flow cytometry of apoptotic cell death. *Journal of Immunological Methods* 243, 167-190 (2000).
119 Bertho, Á. L., Santiago, M. A. & Coutinho, S. G. Flow cytometry in the study of cell death. *Memórias do Instituto Oswaldo Cruz* 95, 429-433 (2000).
120 Darzynkiewicz, Z. & Li, X. in *Flow and Image Cytometry* 115-130 (Springer, 1996).
121 Franzen, J. *et al.* DNA methylation changes during long-term in vitro cell culture are caused by epigenetic drift. *Communications Biology* 4, 598 (2021).
122 Sunila, E. S., Kuttan, R., Preethi, K. C. & Kuttan, G. Dynamized Preparations in Cell Culture. *Evidence-Based Complementary and Alternative Medicine* 6, 296291 (2009).
123 Kato, N. *et al.* Genetic variation and dynamics of hepatitis C virus replicons in long-term cell culture. *Journal of General Virology* 86, 645-656 (2005).
124 Zhao, P. *et al.* A novel multifunctional platform based on ITO/APTES/ErGO/AuNPs for long-term cell culture and real-time biomolecule monitoring. *Talanta* 228, 122232 (2021).
125 Miller, C. N. *et al.* A cell culture platform for Cryptosporidium that enables long-term cultivation and new tools for the systematic investigation of its biology. *International Journal for Parasitology* 48, 197-201 (2018).
126 Xie, X. *et al.* Effects of Long-Term Culture on Human Embryonic Stem Cell Aging. *Stem Cells and Development* 20, 127-138 (2010).
127 Gordon, P. B., Sussman, I. I. & Hatcher, V. B. Long-term culture of human endothelial cells. *In Vitro* 19, 661-671 (1983).
128 Lippman, M., Bolan, G. & Huff, K. The Effects of Estrogens and Antiestrogens on Hormone-responsive Human Breast Cancer in Long-Term Tissue Culture1. *Cancer Research* 36, 4595-4601 (1976).
129 Guan, Z., Jia, S., Zhu, Z., Zhang, M. & Yang, C. J. Facile and Rapid Generation of Large-Scale Microcollagen Gel Array for Long-Term Single-Cell 3D Culture and Cell Proliferation Heterogeneity Analysis. *Analytical Chemistry* 86, 2789-2797 (2014).
130 Liu, M., Miller, C. L. & Eaves, C. J. Human long-term culture initiating cell assay. *Methods in Molecular Biology* 946, 241-256 (2013).
131 Ruhnke, M. *et al.* Long-Term Culture and Differentiation of Rat Embryonic Stem Cell-Like Cells into Neuronal, Glial, Endothelial, and Hepatic Lineages. *Stem Cells* 21, 428-436 (2003).
132 Park, Y. B. *et al.* Alterations of proliferative and differentiation potentials of

human embryonic stem cells during long-term culture. *Experimental & Molecular Medicine* 40, 98-108 (2008).
133 Goldstein, M. N., Burdman, J. A. & Journey, L. J. Long-Term Tissue Culture of Neuroblastomas. II. Morphologic Evidence for Differentiation and Maturation2. *JNCI: Journal of the National Cancer Institute* 32, 165-199 (1964).
134 Ziółkowska, K. *et al.* Long-term three-dimensional cell culture and anticancer drug activity evaluation in a microfluidic chip. *Biosensors and Bioelectronics* 40, 68-74 (2013).
135 Dragoj, M. *et al.* Development and Validation of a Long-Term 3D Glioblastoma Cell Culture in Alginate Microfibers as a Novel Bio-Mimicking Model System for Preclinical Drug Testing. *Brain Sciences* 11, 1025 (2021).
136 Giandomenico, S. L., Sutcliffe, M. & Lancaster, M. A. Generation and long-term culture of advanced cerebral organoids for studying later stages of neural development. *Nature Protocols* 16, 579-602 (2021).
137 Zhao, H. *et al.* Sphere-forming assay vs. organoid culture: Determining long-term stemness and the chemoresistant capacity of primary colorectal cancer cells. *International Journal of Oncology* 54, 893-904 (2019).
138 Kleine-Brüggeney, H. *et al.* Long-Term Perfusion Culture of Monoclonal Embryonic Stem Cells in 3D Hydrogel Beads for Continuous Optical Analysis of Differentiation. *Small* 15, 1804576 (2019).
139 Rodrigues, P. M. & Banales, J. M. Applications of organoids in regenerative medicine: a proof-of-concept for biliary injury. *Nature Reviews Gastroenterology & Hepatology* 18, 371-372 (2021).
140 Geuens, T., van Blitterswijk, C. A. & LaPointe, V. L. S. Overcoming kidney organoid challenges for regenerative medicine. *Nature Partner Journal Regenerative Medicine* 5, 8 (2020).
141 Yin, L. *et al.* Efficient drug screening and nephrotoxicity assessment on co-culture microfluidic kidney chip. *Scientific Reports* 10, 6568 (2020).
142 Pognan, F. *et al.* The evolving role of investigative toxicology in the pharmaceutical industry. *Nature reviews drug discovery* 22, 317-335 (2023).
143 Sart, S., Ronteix, G., Jain, S., Amselem, G. & Baroud, C. N. Cell Culture in Microfluidic Droplets. *Chemical Reviews* 122, 7061-7096 (2022).
144 Büttner, F. H. Cell-based assays for high-throughput screening. *Expert Opinion on Drug Discovery* 1, 373-378 (2006).
145 Geyer, F. L., Ueda, E., Liebel, U., Grau, N. & Levkin, P. A. Superhydrophobic–superhydrophilic micropatterning: towards genome-on-a-chip cell microarrays. *Angewandte Chemie International Edition* 50, 8424-8427 (2011).